

# **Charge Transport in Melanin, a Disordered Bio-Organic Conductor**

**Clare Giacomantonio**

**A thesis submitted for the degree of  
Bachelor of Science with Honours in Biophysics  
University of Queensland**

**June, 2005**



---

# Declaration

---

This thesis is an account of research undertaken between July 2004 and June 2005 at The Department of Physics, Faculty of Engineering and Physical Sciences, University of Queensland, Brisbane, Australia under the supervision of Dr Paul Meredith and Dr Ben Powell.

Except where acknowledged in the customary manner, the material presented in this thesis is, to the best of my knowledge, original and has not been submitted in whole or part for a degree in any university.

---

Clare Giacomantonio  
June, 2005



---

# Acknowledgments

---

This thesis (and I) would not be here if it weren't for the support of many people.

Firstly, of course, my two most-excellent supervisors—Paul Meredith and Ben Powell. I extend my sincerest thanks to both of them for their unfailing faith in me and this project. Their time and support, and their expertise was greatly appreciated.

Also thanks to Andrew Watt for his help with all things physics and Evan Moore for his help with all things chemistry. Thank-you too to Ross McKenzie for his thoughts on various aspects of the theory. And to Shuzhi Cai for his assistance with various things around the lab but especially for taking the SEM images of my samples.

On a more specific note, thanks to: Surya Subianto at the QUT Chemistry Department for his kind donation of some samples; to Chris Vale and Andrew White for the loan of various experimental equipment; and to Paul Bern and Kevin ??? at Oxford for running the TGA on my samples.

And finally, behind the scenes, thanks to my family for getting me this far. I could not have done it without you. To the honours students of 301 for both keeping me sane and driving me insane. And to John Clair for his support and understanding and late-night ice-cream deliveries to the honours room.



---

# Abstract

---

Melanins are biological macromolecules with many roles in the biosphere including as pigments and photoprotects. They have been shown to possess several interesting physical and chemical properties. However, these properties are, in general, poorly understood. This thesis presents a systematic investigation into charge transport physics in melanin. Charge transport-related properties in solid state melanin have been shown to be highly dependent on hydration but these dependencies have been poorly characterised. In this thesis, the relationship between the conductivity of solid-state melanin and hydration is investigated and, for the first time, tied to theoretical predictions on the effects of water on conductivity and interpreted in terms of specific charge transport mechanisms. It is suggested that melanin is a mixed conductor and that the dominant charge carriers change from electrons to protons as hydration increases. Thermogravimetric analysis of melanin suggests that melanin may contain two fractions of water—a strongly bound and a weakly bound fraction. Scanning electron microscopy of two different types of synthetic melanin shows a similar layered structure in both samples. Finally, an attempt at measurement of the proton mobility is outlined.



---

# Contents

---

<b>Declaration</b>	<b>iii</b>
<b>Acknowledgments</b>	<b>v</b>
<b>Abstract</b>	<b>vii</b>
<b>1 Introduction</b>	<b>1</b>
1.1 Background and Motivation . . . . .	1
1.2 Outline . . . . .	1
<b>2 Melanins</b>	<b>3</b>
2.1 Location and Production . . . . .	3
2.2 Properties and Functions . . . . .	4
2.3 Structure . . . . .	5
2.4 Studies of Solid State Properties . . . . .	8
2.5 Summary . . . . .	10
<b>3 Electronic Conduction in Disordered Systems</b>	<b>11</b>
3.1 Amorphous Semiconduction Theory . . . . .	11
3.2 Percolation Theory . . . . .	13
3.3 The Relationship Between the Localisation and Percolation . . . . .	14
3.4 Water and Amorphous Semiconduction Theory . . . . .	15
3.5 Water and Percolation Theory . . . . .	19
3.6 Summary . . . . .	19
<b>4 Effect of Adsorbed Water on Conductivity</b>	<b>21</b>
4.1 Materials and Methods . . . . .	21
4.1.1 Sample Preparation . . . . .	21
4.1.2 Measuring Conductivity at Various Relative Humidities . . . . .	22
4.2 Results . . . . .	25
4.3 Discussion . . . . .	29
4.4 Proposed Conduction Mechanisms . . . . .	32
4.5 Summary . . . . .	34

---

<b>5</b>	<b>Protonic Conduction</b>	<b>35</b>
5.1	Mechanisms of Proton Conduction . . . . .	35
5.2	The Effect of Water on Conductivity . . . . .	36
5.3	Protonic Conduction in Percolated Systems . . . . .	37
5.4	Experimental Evidence . . . . .	38
5.5	Mixed Conductors . . . . .	39
5.6	Summary . . . . .	39
<b>6</b>	<b>Charge Transport in Biological Macromolecules</b>	<b>41</b>
6.1	Collagen . . . . .	41
6.2	Lysozyme . . . . .	42
6.3	Melanin . . . . .	42
6.3.1	The Story So Far . . . . .	42
6.3.2	A Case for Protonic Conduction in Melanin . . . . .	43
6.4	Summary . . . . .	45
<b>7</b>	<b>Re-examining the Effect of Adsorbed Water on Conductivity</b>	<b>47</b>
7.1	Proposed Conduction Mechanisms Revisited . . . . .	47
7.2	Comparison with Experiments . . . . .	50
7.3	Modelling with Equivalent Circuits . . . . .	50
7.4	Summary . . . . .	54
<b>8</b>	<b>Scanning Electron Microscopy and Thermogravimetric Analysis</b>	<b>55</b>
8.1	Scanning Electron Microscopy . . . . .	55
8.1.1	Materials and Methods . . . . .	55
8.1.2	Results and Discussion . . . . .	55
8.2	Thermogravimetric Analysis . . . . .	58
8.2.1	Materials and Methods . . . . .	58
8.2.2	Results and Discussion . . . . .	58
8.3	Summary . . . . .	61
<b>9</b>	<b>Charge Carrier Mobility</b>	<b>63</b>
9.1	Materials and Methods . . . . .	63
9.1.1	Sample preparation . . . . .	63
9.1.2	Measuring Mobilities . . . . .	63
9.2	Results and Discussion . . . . .	65
9.3	Summary . . . . .	66
<b>10</b>	<b>Conclusions</b>	<b>69</b>
10.1	Further research . . . . .	69
10.2	Conclusions . . . . .	70
	<b>References</b>	<b>73</b>

---

# Introduction

---

## 1.1 Background and Motivation

Organic conductors are an interesting class of materials already being used in many different technological applications including photovoltaics, sensors and other electronic devices. Disordered organic conductors and semiconductors also exhibit interesting properties giving them potential for technological uses. However, these properties, including the charge transport mechanism, are generally poorly understood.

The biopolymer melanin is a disordered bio-organic conductor. Its unique physical and chemical properties confer a broad range of functions in nature, including roles as a photoprotectant, pigment, charge transport mediator, free radical scavenger and antioxidant.

In order to utilise melanin's unique properties in making novel or improved functional materials, the charge transport mechanism in melanin must first be fully characterised. Through investigation of the charge transport mechanism of melanin, insight into the workings of other disordered organic conductors may also be gained. Additionally, as melanin is a biological molecule, characterisation of its charge transport mechanism may also provide a greater understanding of its biofunctionality and role in disease.

Many physical properties related to charge transport in melanin have been shown to be affected dramatically by adsorbed water. This suggests that water plays a significant role in the charge transport mechanism in melanin and raises the possibility that the majority charge carriers may be ions or protons rather than electrons.

This thesis aims to begin the process of solving the charge transport mechanism mystery in melanin by reviewing possible mechanisms and discussing new experiments related to charge transport.

## 1.2 Outline

We begin in chapter 2 with an overview on melanin's synthesis, structure, properties and functions. This chapter also gives a review of the literature on charge transport-

related properties in melanin. This chapter should give the reader an idea of the current state of melanin research and the motivations behind this thesis.

Chapter 3 then outlines the theories of electronic conduction in amorphous systems and explores the theories behind how water can affect electronic conduction in these systems.

Chapter 4 is an experimental chapter detailing our experiments characterising the relationship between adsorbed water and dark DC conductivity in melanin. In this chapter, the results of this experiment are analysed in the context of the already presented theories on electronic conduction in disordered systems. On the basis of agreement with theory at low hydration, an electronic conduction mechanism is proposed in this regime. It is suggested that electronic conduction cannot explain the results of this experiment at high hydration.

Motivated by the results of the conductivity experiment, the next chapter—chapter 5—outlines the theory of protonic conduction in hydrated systems and ways in which proton conductors can be identified experimentally.

Chapter 6 then reviews the literature on charge transport in other biological macromolecules and makes a case for protonic conduction in melanin based on results from the existing literature.

The results of the conductivity experiment are then re-discussed in chapter 7 in light of the theories and literature on protonic conduction presented in the preceding two chapters. A qualitative agreement with some of the theory of protonic conduction in hydrated systems leads us to suggest that in hydrated melanin, conduction may be via protons along disordered networks of hydrogen-bonded water molecules. We also observe that some interaction between the two conduction mechanisms must exist if our conductivity results are to be completely explained.

Chapter 8 details scanning electron microscopy and thermogravimetric analysis of our samples. Scanning electron micrographs reveal structural similarities between the two different types of synthetic melanin used in the conductivity experiment. This helps us to explain similarities in the measured properties of the two samples. Meanwhile, thermogravimetric analysis of our samples shows that adsorbed water may make up about 50% of the weight of hydrated melanin and this water may consist of a strongly bound and a loosely bound fraction.

In the final experimental chapter, an experiment designed to measure the mobility of protons in melanin as a function of hydration is presented and discussed. The measured proton mobilities are found to be very high and so may not be representative of the true proton mobility in melanin.

And finally, in the conclusion (chapter 10) we summarise the main findings of this thesis and suggest some possible next steps in melanin research to extend and explore the ideas generated in this thesis.

---

# Melanins

---

For all complex biological macromolecules, particular structural features confer particular properties that in turn allow the molecules to perform specific functions within an organism. Despite extensive research, there are many unanswered questions about the structure-property-function relationships of melanins. This was well expressed by Blois [2], who wrote in 1978:

*From the early commentary by Aristotle (315 B.C.) to the most recent investigations, the study of melanins has involved virtually every applicable chemical and physical technique, and the motivation in this research has reflected the biological fashion of each era. Notwithstanding these efforts, we still do not know their chemical structure or molecular weights, their mode of synthesis is not yet agreed upon, a satisfactory nomenclature remains to be devised, and even their biological role is more a matter of surmise than proof.*

Since 1978, researchers have continued to apply new techniques to the study of melanin to help solve some of melanins' mysteries, but many gaps in our understanding still remain. The physical and electronic structure of melanin remains essentially unknown and many unusual properties remain uncharacterised.

This chapter gives a brief overview of what melanin is, where it is made in the human body and some of its hypothesised structure-property-function relationships. As this thesis is particularly concerned with charge-transport, an extensive review of studies on properties of melanin relating to this particular subject is also given.

## 2.1 Location and Production

Melanins are a class of dark biological pigments found in the skin, hair, eyes, inner ears and brain-stems of many species including humans. There are two main types of melanin: eumelanins which are brown-black pigments and pheomelanin which is a yellow-red pigment. Eumelanin is the more common form and is the type studied in this thesis.

It is thought that eumelanins are synthesised *in vivo* by the enzymatic metabolism of the amino acid tyrosine into 5,6-dihydroxyindole (DHI) and 5,6-dihydroxyindole-2-carboxylic acid (DHICA) in a process known as melanogenesis [3] illustrated in figure 2.1. Melanogenesis occurs in specialised organelles known as melanosomes within specialised cells, the most common being the melanocytes located in the epidermis of higher vertebrates.[3] Pathological disorders related to melanin production include albinism and melanoma.[3]

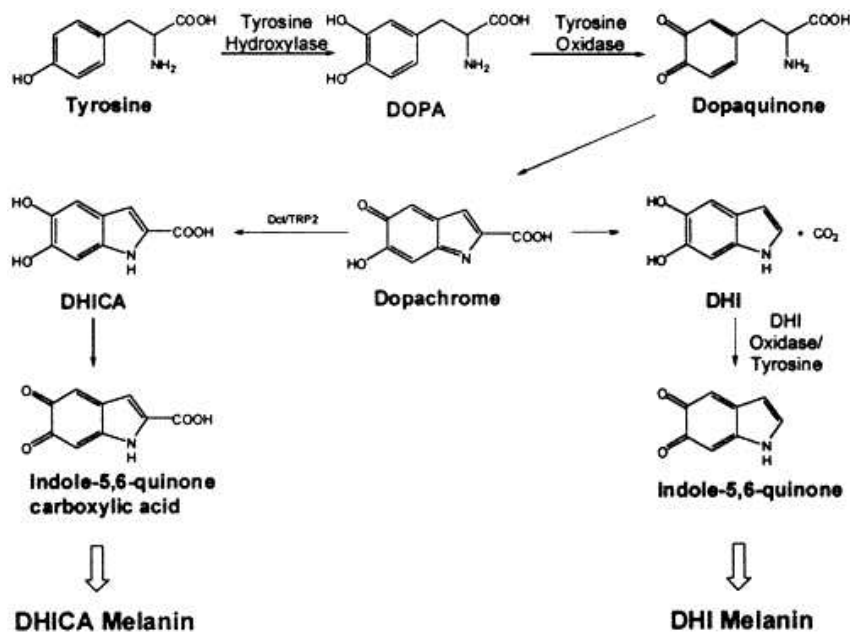


**Figure 2.1:** The biosynthetic pathway of DHI and DHICA eumelanins. Natural melanin is formed from a mixture of DHI and DHICA precursors. Taken from [4].

## 2.2 Properties and Functions

Melanins have several interesting properties which accord many functions, the main two functions being a photoprotector and pigment.

Broad-band UV-visible absorbance characteristics allow melanins to function as photoprotectants. Such broad-band absorbance is very unusual for biomolecules and the actual mechanisms by which melanins absorb and dissipate energy are not yet understood. In paradox with its function as a photoprotectant, melanin is also implicated in melanoma formation.[3]

As a pigment, melanins are responsible for some of the coloured patterns in the hair and skin of many vertebrates.[3] This pigmentation can be of importance in

both natural and sexual selection. In cuttlefish, *Sepia officinalis*, eumelanin is the pigment that colours the ink they release.

Melanins also serve as free radical scavengers, antioxidants and photoconductors. The function of the melanin located in the brain-stem and inner ear is poorly understood.

## 2.3 Structure

It is generally accepted that eumelanins consist of mainly DHI and DHICA monomer units (seen in figure 2.1), with polymerisation points shown in figure 2.2.[3] These monomers are thought to link randomly with each other and some precursors to form oligomers and polymers. The monomer molecules can be in various oxidation states as seen in figure 2.2. As a result, melanin is not a conventional, single, well-defined molecule, but rather, a heterogeneous mixture of similar macromolecules made from random linkages of these basic structural units. *In vivo*, melanins also exist intermixed with other molecules such as proteins.

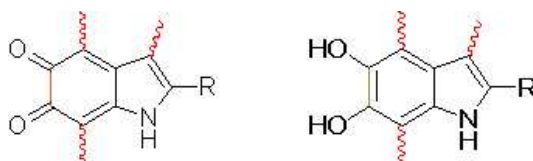


**Figure 2.2:** The building blocks of eumelanin. R represents a COOH group in DHICA and a H in DHI. Squiggly lines indicate sites of attachment to the extended polymer and possibly to proteins. The details of these attachments in the total complex structure are not known.

The main debate surrounding the overall structure of melanin is whether these oligomers form extended heteropolymers, as seen in figure 2.3, or nanoaggregates, as seen in figure 2.4. In the nanoaggregate picture, it is proposed that approximately five monomer units link together to form small planar oligomers. These oligomers may then assemble via  $\pi$  stacking into nanoaggregates of three to four layers. Nanoaggregates can then cluster together via side-on interactions such as hydrogen bonding as illustrated in the bottom left of figure 2.4. The nanoaggregate model is supported by x-ray scattering [5, 6] and atomic force microscopy [4] studies. The atomic force microscopy study by Clancy and his associates [4] also revealed some filament structures. A possible explanation for these structures is illustrated in the bottom right of figure 2.4

The idea of a biomolecule with a structure based upon heterogeneity or disorder is a large break from the central dogma of structural biochemistry where all molecules have a very well defined structure. It is this disorder that makes the mod-

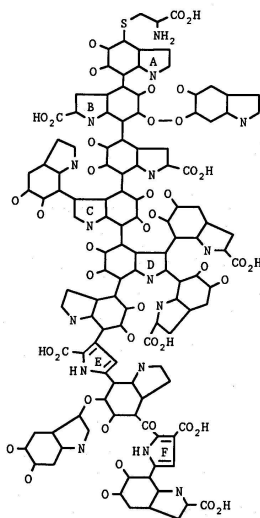


**Figure 2.3:** The extended heteropolymer model of eumelanin structure. Here, six indole monomer units (A-F) form a randomly linked polymer. The monomer units may be in various oxidation states. Taken from [3].

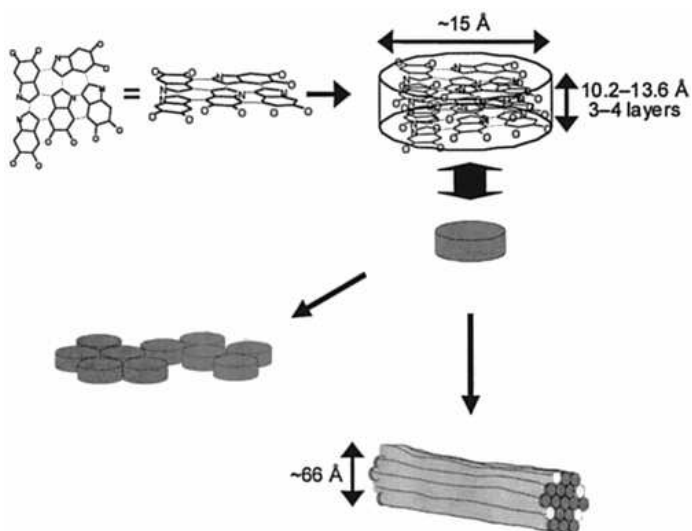


**Figure 2.4:** The nanoaggregate model of eumelanin structure. About 5 DHI/DHICA units link randomly to form an approximately planar oligomer. The oligomers then assemble via  $\pi$  stacking into nanoaggregates. Nanoaggregates can form clusters via side-on interactions (bottom left) or filaments (bottom right). Taken from [4].

ern approaches of spectroscopy and x-ray diffraction analysis, which have been used so successfully to elucidate the structure of other complex bio-macromolecules, so ineffective for the study of melanins.[3]

Nonetheless, the idea of a structure based on disorder does not necessarily break with the structure-property-function paradigm of structural biochemistry. Indeed, it is the disordered structure which may give melanin many of its interesting properties. For example, energy minimised density functional theory calculations [7, 8, 9] and molecular dynamics simulations [10] have suggested that the monotonic broad-band absorbance of melanin may be attributed to a large ensemble of different monomers and oligomers, each with a slightly different absorption peaks. Figure 2.5(a) shows the absorption spectra of a single hexamer sheet in various oxidation states. Stacking of the sheets and environmental factors also broaden and shift the peaks. It is proposed that with enough of this chemical disorder, the overlapping individual peaks would be smeared into the monotonic absorption spectrum observed experimentally (figure 2.5(b)).[8, 11]

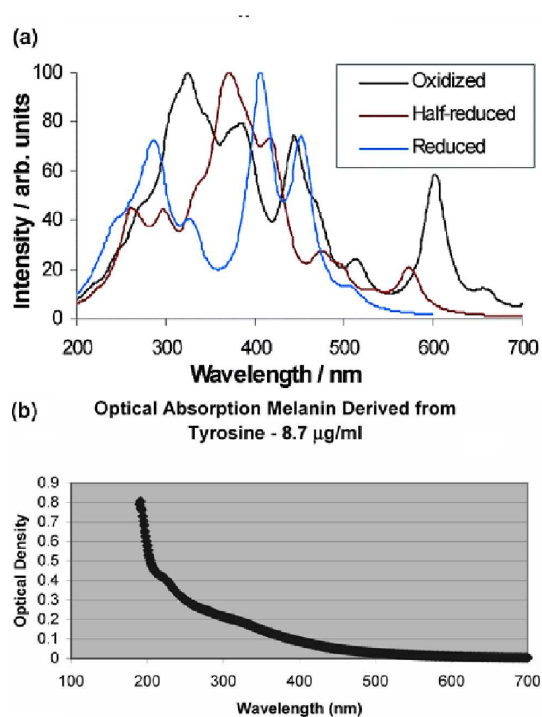


**Figure 2.5:** The absorption spectrum of eumelanin. (a) Theoretical prediction of the spectra of individual single hexamer sheets in different oxidation states. Taken from [10]. (b) The experimentally observed monotonic broad-band spectrum. Taken from [9]. The existence of different size sheets and environmental factors may smear the theoretical prediction to more closely resemble the experimentally observed spectrum.[9, 10, 11]

## 2.4 Studies of Solid State Properties

Numerous studies investigating various properties of solid state melanin have been published. Some of these studies examine properties which are related to charge transport mechanisms. Of these studies, most have shown that water plays a fundamental role in defining many of the physical properties of melanin and hence, that water must play a fundamental role in the charge transport mechanism. However, despite the significant effect of water, most studies investigating properties related to charge transport were performed without proper hydration control. Additionally, few studies seriously attempted to tie their observations to particular charge transport mechanisms.

As far back as 1974, McGinness, Corry and Proctor [12] reported a room temperature DC conductivity of melanin of  $10^{-5}$  S/cm, suggesting that melanin may be a semiconductor. They also reported a switching behaviour similar to that observed in some inorganic amorphous semiconductors. Meanwhile, in 1979 Baraldi *et al.* [13] reported a room temperature conductivity of  $10^{-12}$  S/cm, calculated from the steady state current measured five minutes after the electric field was applied. While both these studies recognised that removing water by heating the sample dramatically affected the conductive properties, the hydration levels of the samples during measurements were not reported. Different hydration levels and settling times are the likely causes of the large difference between the two conductivities.

The significant effect of water on the electrical properties of melanin was also recognised in thermally stimulated depolarisation current (TSDC) measurements.[13, 14] These studies showed that melanin may have an intrinsic polarisation, giving a large TSDC in samples not previously submitted to thermal treatment. When the samples were subjected to a polarising field before measurements, four main current peaks were detected [14]. Each of these peaks was shifted and diminished significantly in intensity by heating. These results indicate that TSDCs in melanin are caused by the release or reorientation of water molecules. The properties of two of the peaks suggested the presence of two types of water in melanin — an “easy” water and an ice-like “hard” water.

Differential scanning calorimetry (DSC) curves for melanin also demonstrated the importance of water [15]. The curves showed an endothermal drop at about 320K which is indicative of a phase transition. Simonovic *et al.* postulated that water molecules may be present between the graphite-like stacked planar layers thought to be present in melanin. These water molecules may bind directly to each other and melanin. During heating, the breaking of these bonds may displace the stacked layers causing a phase transition evident as an endothermal drop. Cooling may return the sheets to their original positions. When heating runs were performed in quick succession, a smaller change in enthalpy, credited to water desorption, was observed. The size of the endothermal drop recovered to its original value when a large length of time was allowed to lapse between successive runs, as water was

readsorbed.

Dielectric spectroscopy of pressed synthetic melanin powders showed two relaxation regions.[16] These were attributed to two main hopping distances for water-assisted hopping polarization. An increase in the hopping distances upon heating was attributed to a decrease in hydration.

In the conductivity, TSDC, DSC and dielectric studies cited, water levels were changed by heating but quantitative measurements of hydration were not attempted. All studies used either synthetic melanin or a combination of synthetic and extracted natural melanin in the form of loose or pressed powders. The main concern with powder samples is that they are unlikely to be representative of the proposed layered structure of natural melanin.

Quantitative control of the hydration level in order to characterise its effect on the conductivity of melanin was performed by Jastrzebska *et al.* in 1995.[1] Humidity levels were controlled by placing the samples in equilibrium with various saturated salt solutions. In general, conductivity was found to vary exponentially with the humidity, showing an increase from about  $10^{-10}$  S/cm to  $10^{-5}$  S/cm for a humidity rise from 3 to 100% relative humidity as seen in figure 2.6. In a 0.04 mb vacuum, the conductivity deviated from the extrapolated expected value of  $10^{-11}$  S/cm to a much lower value of  $10^{-13}$  S/cm suggesting that dry melanin may be an insulator. In the same study, conductivity under vacuum was found to vary with temperature according to the Arrhenius equation which is characteristic of semiconductor materials. However, this result should be viewed with caution as the temperature range of about 21 to 50°C is really too narrow to allow solid conclusions to be made. Samples in this study were pressed powders of synthetic melanin.

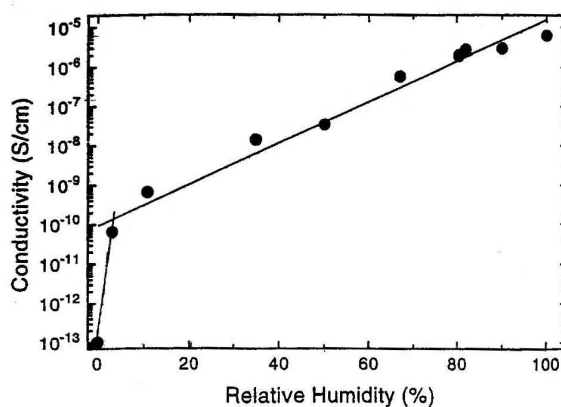


**Figure 2.6:** Conductivity of solid state synthetic melanin as a function of relative humidity. Sample was a pressed pellet of melanin powder 1 mm thick and 5 mm in diameter. Taken from [1].

Photoconductivity measurements on natural melanins showed that the amplitude of the photocurrent increased by more than one order of magnitude with an increase in hydration from 3 to 40 weight percent adsorbed water.[17]

All the solid state studies cited so far examine various properties related to charge transport in melanin. All show that water content significantly affects these properties. However, none attempt to interpret their observations in detail in terms of a specific charge transport mechanism. McGinness *et al.* advocate the alteration of melanin's dielectric constant (for conducting in the switched on state) while Bridelli *et al.* propose some of their results may be interpreted in terms of a proton migration process. Meanwhile, Jastrzebska *et al.* suggest their findings are in qualitative agreement with small polarons as the charge carriers. However, these interpretations are added almost as afterthoughts to studies using methods which do not definitively advocate a particular conduction mechanism over the other. Additionally, results of these studies often have more than one equally valid interpretation in terms of different conduction mechanisms, as we will see in chapters 5 and 6.

## 2.5 Summary

We have seen that despite extensive research, many questions about the structure, properties and functions of melanin remain. In particular, the charge transport mechanism in melanin is completely unknown as most studies of properties relating to transport cannot be used to elucidate mechanistic information because hydration was not controlled.

Motivated by this current situation, this thesis aims to start to unravel the charge transport mechanism mystery by reviewing possible mechanisms and discussing experiments we performed relating to charge transport, with hydration control.

---

# Electronic Conduction in Disordered Systems

---

As stated in chapter 2, melanins are generally accepted to be structurally disordered. For this reason, the theory of electronic conduction is presented in this chapter in the context of amorphous systems. Both amorphous semiconduction theory and percolation theory are outlined and the relationship between the two theories is discussed. Theories on the effect of water on electronic conductivity are presented in both the amorphous semiconduction and percolation pictures of electronic conduction in disordered systems.

## 3.1 Amorphous Semiconduction Theory

In crystalline materials, long-range periodicity of the materials' constituent atoms results in the formation of extended energy bands through which delocalised electrons can move freely. These bands are the allowed energy states of the electrons given by the solution to Schrodinger's equation in an appropriate spatially periodic potential.[18] In semiconductors, the extended states form two bands: a valence band and a conduction band, which are separated by an energy gap known as the band gap. This is illustrated in figure 3.1(a). Both electrons in the conduction band and holes in the valence band are capable of conduction. In intrinsic semiconductors, electrons are thermally excited into the conduction band leaving holes in the valence band. In extrinsic semiconductors, donor or acceptor atoms are introduced into the lattice interstitially or by substitution. Donors supply additional electrons to the conduction band while acceptors capture electrons from the valence band leaving holes as seen in figure 3.1(a).

In amorphous systems, the theory underlying electronic conduction is qualitatively different owing to the absence of structural periodicity. In particular, this departure from regularity causes states to become localised. In partially disordered systems, the localised states may form tails extending from the valence and conduction band edges into the band gap as illustrated in figure 3.1(b).[19]. These states

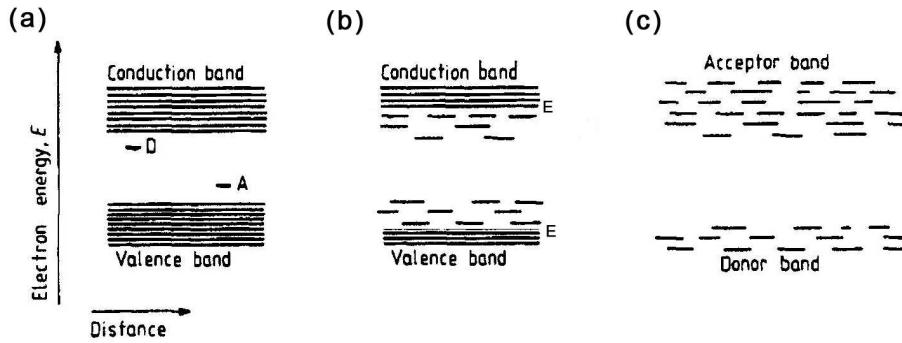


**Figure 3.1:** Electron energy states in (a) a crystalline semiconductor, (b) a partially disordered semiconductor and (c) a truly amorphous semiconductor. In (a), extended states form a conduction and a valence band while donor atoms  $D$  and acceptor atoms  $A$  donate and accept electrons respectively. In (b), localised states extend from the band edges into the band gap.  $E$  are the mobility edges. In (c) there are no extended states but localised states can form ‘pseudobands’. Modified from a figure in [18].

span a continuous range of energies from the edge of the band gap up or down to critical energies, known as the mobility edges, where the states become extended.[19] In completely amorphous materials, there may be no extended states as seen in figure 3.1(c).

If extended states exist and if the Fermi energy lies below the mobility edge of a partially amorphous system, then conduction occurs via either thermal excitation above the mobility edge or thermally activated hopping between the localised states across intervening potential barriers.[19] In the second case, the rate of transfer depends on the size of the potential barriers and the extent of overlap of the electron wavefunctions, which depends on the site separation.[18] In a completely amorphous system, conduction must occur via hopping.

The rate of hopping is also dependent on interactions between each site and its environment.[18] For example, in a material with strong phonon-coupling with the surrounding medium, the energy necessary to transverse the potential barrier may be provided by phonons, leading to a higher transfer rate. In biological macromolecules, interactions with surrounding molecules such as water and ions are particularly important as biomacromolecules exist *in vivo* in hot and wet mixtures of many different molecules and ions. These interactions can alter the energies of localised states, which may increase or decrease the transfer rate.

In general, conductivity in both crystalline and amorphous semiconductors varies

with temperature  $T$  according to the Arrhenius equation

$$\sigma = \sigma_0 \exp\left(\frac{-E_A}{kT}\right) \quad (3.1)$$

where  $\sigma_0$  is a constant of the material,  $E_A$  is the activation energy for semiconduction and  $k$  is Boltzmann's constant.

## 3.2 Percolation Theory

Percolation theory is an alternative theory explaining conductivity in amorphous solids.[20, 21, 22] It is commonly used more generally to explain the properties of systems of randomly connected elements such as the flow of liquids in porous media.

The easiest introduction to percolation theory is through a simple example taken from [20]. We consider an electrical network based on the network seen in figure 3.2(a). Each copper strand is either intact (and therefore conducting) or cut (and therefore insulating). The cutting of copper strands is random. The strands on the left and right are connected to two copper bars and a voltage is applied across the two bars. It can be shown experimentally and theoretically that the conductivity of the network as a function of the probability of a site being occupied has the form of figure 3.2(b).[21, 22]

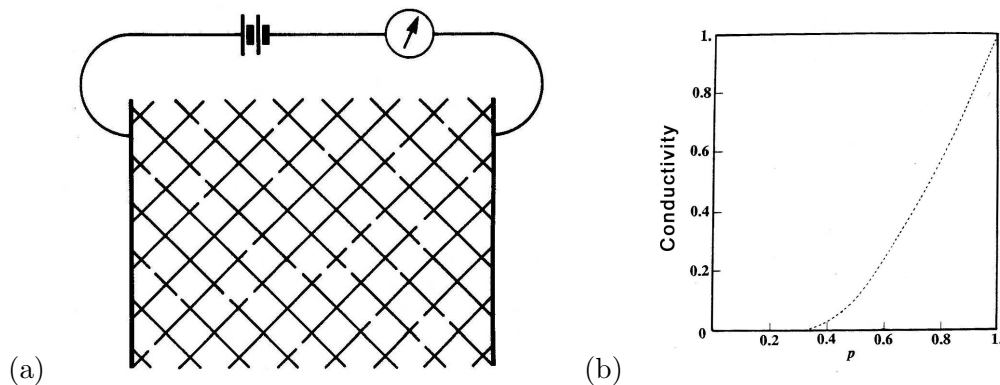


**Figure 3.2:** Percolated conductivity. (a) A random copper strand network. Copper strands are either intact or cut. The conductivity of the network can be calculated from the current flowing through the network as a result of a voltage applied across it and the dimensions of the network. Taken from [20]. (b) The conductivity of a random conductor network as a function of the probability  $p$  of a conductor strand being intact. Modified from a figure in [22].

In this example, the random conductor network is a percolated system. The

relationship between the conductivity and the probability of a bond being intact  $p$  can be explained using percolation theory. Until some critical probability  $p_c$  known as the percolation threshold, there is no flow of current as there is no continuous path from the left bar to the right bar. At the percolation threshold, long-range connectivity suddenly occurs. Past the percolation threshold, more and more pathways form between the two bars, increasing the conductivity. Immediately past the percolation threshold, conductivity increases slowly as some of the additional copper strands are added to dead ends and so do not help increase the conductivity. As the probability of a bond being intact increases further, former dead ends become current-carrying pathways resulting in the power-law relationship between the conductivity and the intact-bond probability seen in figure 3.2. The critical probability  $p_c$  depends on the properties of the conductor and the geometry of the network.

The discussion so far has described bond percolation. It has a counterpart known as site percolation where the network now consists of sites which are either occupied with probability  $p$  or unoccupied.

The quantitative form of the relationship between the conductivity and probability of a bond being intact or a site being occupied is the percolation equation

$$\sigma = (p - p_c)^\mu \quad (3.2)$$

where the critical exponent  $\mu$  is 1.3 for a two dimensional system and 2.0 for a three dimensional system.[22]

### 3.3 The Relationship Between the Localisation and Percolation

So far in this chapter, two theories dealing with charge transport in disordered systems have been outlined. The differences between the two theories lie in the scale of the disorder.[20]

Localisation theory is concerned with microscopically disordered but macroscopically homogeneous systems. The important feature of this theory is that microscopic disorder results in localised states. To conduct in these systems, electrons must hop between localised eigenstates or be excited above the mobility edge into the extended eigenstates. The concern with the energy states of the system makes this theory a quantum problem.

Percolation theory deals with macroscopically inhomogeneous systems. In this theory, the nature of the energy levels does not matter. Hence, the presence or absence of microscopic disorder is irrelevant. As long as some elements within the material conduct, we are only concerned with how the conducting elements are related to each other, not the mechanism of conduction. As a result, percolation theory is equally applicable to electronic conductors and semiconductors and protonic conductors (as we shall see in chapter 5). The percolation problem is essentially a

classical probability problem.[23]

### 3.4 Water and Amorphous Semiconduction Theory

The effect of water on conductivity is given special consideration as most biological processes occur in aqueous environments. Moreover, water has been shown experimentally to have a dramatic effect on the conductivity of many biomacromolecules. Theoretically, water could affect electron transfer processes in two complementary ways: by ionisation of acidic and basic groups or by modifying the local dielectric constant of the material.

When materials are exposed to water vapour, they adsorb water molecules onto their surfaces. These surfaces include not only the external surfaces, but also internal surfaces such as the insides of pores and the surfaces between layers. At all surfaces, the water molecules are able to interact strongly with molecules of the solid, giving water the potential to greatly affect the properties of the condensed phase.

It should be noted that the theories on how water affects conductivity presented in this section do not rely on the theory of amorphous systems. This suggests that water may affect crystalline systems in an equivalent manner. However, for water (or other high dielectric constant materials) to have a dramatic effect, a significant number of semiconductor molecules must be in close proximity to water molecules. In amorphous and partially crystalline solids this is possible as water can be distributed throughout the bulk of the solid. It is generally not possible in crystalline systems because hydration is limited to the external faces of the sample in most cases. As a result, water is not thought to significantly affect the bulk conductivity of most crystalline materials.

One way water can affect conductivity is by reacting with ionisable groups of the constituent material to directly alter the energies of localised states. For example, acid groups can react with water as seen in figure 3.3. There is some suggestion that this may increase the energy of an electron in the  $\text{-COO}^-$  group to just below the conduction band edge, allowing  $\text{-COO}^-$  groups to act as electron donors.[24] Alternatively, the localised charges resulting from the ionisation of basic and acidic groups could simply alter the energy band structure by either attracting or repelling nearby localised electronic states.[24]

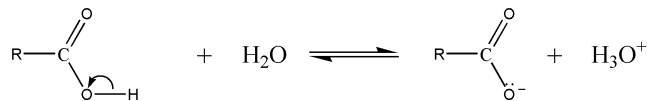


**Figure 3.3:** The ionisation of an acid group by reaction with a water molecule. Position of the equilibrium depends on the strength of the acid. For a strong acid, the equilibrium lies completely to the right.

Even without chemically reacting with the material, water can modify the energies of local electronic states by inducing polarisation. As water molecules are highly polar, water has a high dielectric constant. As a result, when water is adsorbed onto a low dielectric constant material, it increases the effective dielectric constant of the material [25] which, in turn, increases the polarisability of the material. The first contact layers of water interact strongly with the material causing donor states to be increased in energy by the polarisation energy, and acceptor states to be decreased in energy by the polarisation energy [18] thus narrowing the band-gap as seen in figure 3.4.

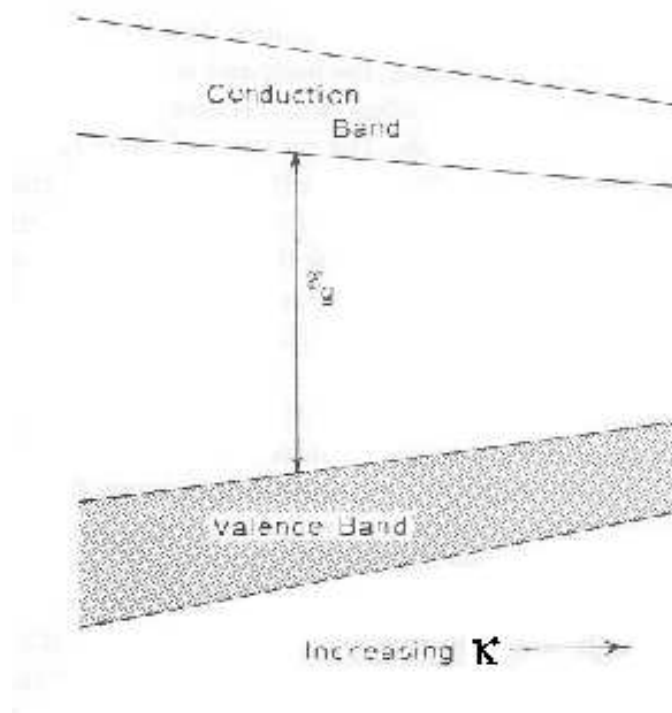


**Figure 3.4:** The change in the energy bands as a function of the dielectric constant  $\kappa$ .  $\epsilon_g$  is the energy of the band gap. Modified from a figure in [24].

A theory relating the effect on the dielectric constant directly to the conductivity was developed by Rosenberg in a study on the conductivity of the protein haemoglobin.[26] A good coverage of this theory is also given in Pethig's book *Dielectric and electronic properties of biological materials*. [24] To develop this model we consider an electron being moved from one originally neutral macromolecule (or part thereof) and placed on another originally neutral macromolecule in a dry

environment. The energy  $E_D$  required to accomplish this is

$$E_D = (I - P^+) - (A + P^-) \quad (3.3)$$

where  $I$  and  $A$  are the ionisation energy and electron affinity of the isolated macromolecule.  $P^+$  and  $P^-$  are the energies of polarisation resulting from the interactions of the positive charge on the donor macromolecule and the negative charge on the acceptor macromolecule, with surrounding macromolecules.

The parameters  $P^+$  and  $P^-$  can be evaluated by considering the electrostatic self-energies of the macromolecular ions. If we approximate the ions as spheres, then the self-energy of an ion in isolation is

$$U_0 = \frac{q^2}{8\pi\epsilon_0 R}. \quad (3.4)$$

If an ion is now embedded in a macromolecule matrix of dielectric constant  $\kappa$ , the electrostatic self-energy decreases to

$$U_M = \frac{q^2}{8\pi\kappa\epsilon_0 R}. \quad (3.5)$$

The difference between these two energies must necessarily be the energy due to interactions of an ion with its environment—the polarisation energy. Therefore,

$$P^+ = P^- = U_0 - U_M = \frac{q^2}{8\pi\epsilon_0 R} \left(1 - \frac{1}{\kappa}\right). \quad (3.6)$$

Hence, for a dry macromolecule

$$E_D = I - A - \frac{q^2}{4\pi\epsilon_0 R} \left(1 - \frac{1}{\kappa}\right). \quad (3.7)$$

As the macromolecule is hydrated, the dielectric constant increases from  $\kappa$  to  $\kappa_w$ . As a result, the parameters  $P^+$  and  $P^-$  also increase, causing a decrease in the energy required to separate the charges. The new energy required to separate the charges is

$$E_W = I - A - \frac{q^2}{4\pi\epsilon_0 R} \left(1 - \frac{1}{\kappa_w}\right) \quad (3.8)$$

Substituting in equation 3.7 gives

$$E_W = E_D - \frac{q^2}{4\pi\epsilon_0 R} \left(\frac{1}{\kappa} - \frac{1}{\kappa_w}\right) \quad (3.9)$$

Substituting this activation energy into the Arrhenius equation 3.1 gives the Rosen-

berg equation for the conductivity of a hydrated macromolecule

$$\sigma_W = \sigma_0 \exp \left[ \frac{-E_D}{kT} \right] \exp \left[ \frac{q^2}{4\pi\epsilon_0 kTR} \left( \frac{1}{\kappa} - \frac{1}{\kappa_w} \right) \right] \quad (3.10)$$

The Rosenberg equation displays an interesting characteristic. As the water content increases (thereby increasing the dielectric constant), the  $\frac{1}{\kappa_w}$  term becomes negligibly small compared to the  $\frac{1}{\kappa}$  term. This means that as the water content increases, the conductivity should tend toward some saturated value for any fixed temperature as illustrated in figure 3.5.

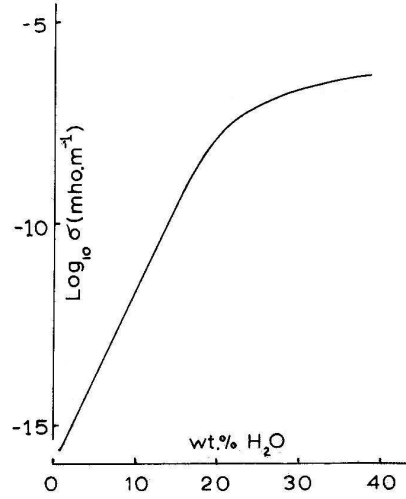


**Figure 3.5:** The variation of the DC conductivity with the hydration of a macromolecule as predicted by equation 3.10. Taken from [24].

It should be noted that as the Rosenberg equation 3.10 was derived using the Arrhenius equation 3.1, it is only applicable to materials in which Arrhenius behaviour is observed. And although Arrhenius behaviour has been observed in many biomacromolecules, its validity is not well established as the temperature ranges over which conductivities have been measured are generally very narrow.

Further insight into the Rosenberg equation 3.10 can be gained by rearranging it into the form

$$\sigma = \sigma_0 \exp \left[ \frac{-(E_D - c)}{kT} \right] \quad (3.11)$$

where

$$c = \frac{q^2}{4\pi\epsilon_0 R} \left( \frac{1}{\kappa} - \frac{1}{\kappa_w} \right). \quad (3.12)$$

When the hydration level is constant,  $c$  is constant. In a dry environment,  $\kappa_w = \kappa$

---

so  $c = 0$ . Comparing equations 3.11 and the Arrhenius equation 3.1 for this case, we see that  $E_D$  is simply the activation energy of the dry macromolecules as expected. As hydration increases,  $c$  also increases causing the activation energy to decrease. In this way, we see that the increase in dielectric constant with hydration manifests itself as a narrowing of the bandgap for semiconduction.

### 3.5 Water and Percolation Theory

Percolation theory relies on forming conducting pathways between previously isolated conducting elements or adding conducting elements to an insulating matrix. As a result, for water to have the effect predicted by equation 3.2, water molecules must form conducting bonds (bond percolation) or be conducting elements (site percolation).

If water is to affect electronic conduction in the bond percolation picture, the water molecules must form electron conducting bonds between electron conducting elements already in place. In general, this does not occur. Although water may connect elements with hydrogen bonds, these bonds do not assist electron transport. In fact, in many materials, water breaks rather than forms bonds conducive to electronic conduction. For example, water can disrupt hydrogen-bonded  $\alpha$ -helical structures in proteins.[27] In general, water is the ubiquitous breaker of dispersive bonds like van der Waals bonds, hydrogen bonds and  $\pi - \pi$  interactions.[27]

On the other hand, it is possible for water molecules to be conducting elements that form a random conductor network in the site percolation picture. Water molecules can form hydrogen-bonded networks but these networks cannot conduct electrons. Instead, the charge carriers in hydrogen-bonded water networks are protons. This possibility and the mechanisms by which protons conduct are discussed further in chapter 5.

### 3.6 Summary

We have already stated that melanins are believed to be structurally disordered. In this chapter, we have not only shown that electronic conduction in disordered systems is possible but also presented two alternative theories of conduction. The first theory, amorphous semiconduction theory, deals with microscopically disordered systems while the second theory, percolation theory, deals with microscopically or macroscopically disordered systems. We have also shown that adsorption of water may increase electronic conductivity by increasing the local dielectric constant. Alternatively, water molecules may form random conductor networks giving percolated protonic conductivity.



---

# Effect of Adsorbed Water on Conductivity

---

As stated in chapter 2, water has been shown to have a very dramatic effect on the physical properties of melanin, but these effects have generally not been quantified. In this chapter, we discuss our experiment characterising the conductivity of melanin as a function of hydration. Our motivations for doing this experiment were two-fold. Firstly, we wished to compare our results with the results of the similar study by Jastrzebska *et al.* [1] discussed in chapter 2. Secondly, we wished to examine two different types of synthetic melanin: pressed powders similar to those used in most melanin studies and thin films. These thin films are a novel form of synthetic melanin thought to be structurally closer to natural melanin.[28] Unlike previous studies, the results of our experiment are discussed in terms of specific charge transport mechanisms—those outlined in chapter 3 for conduction in disordered systems.

## 4.1 Materials and Methods

### 4.1.1 Sample Preparation

#### Synthetic Melanin Films

Following the method of Subianto [28], thin films of synthetic melanin were produced by oxidative electropolymerisation of dl-DOPA (3,4-dihydroxyphenylalanine) (used as received from Sigma-Aldrich). The initial solution was 50 mM of dl-DOPA in sodium tetraborate buffer (Sigma-Aldrich, 0.1 M, pH 9). Current was passed through the solution by dropping a voltage of up to 20 V across a copper cathode and indium tin oxide anode using a PHY-EWS-89 30 V power supply. A CIE 125 digital multimeter was used to measure the current flowing through the circuit.

To accelerate the formation of melanin, the solution was initially oxidised by mechanical stirring for 10 to 15 minutes at a voltage producing 10-20 mA/cm<sup>2</sup> of current. During oxidation, orange dopachrome forming at the anode spread throughout the solution. The solution was then left in atmospheric conditions at a current

density of 0.4-0.5 mA/cm<sup>2</sup> for 9 days. During this time, the solution turned black and a soft black melanin film up to approximately 1 mm thick formed on the anode.

Once thick enough, the film was separated from the anode with a scalpel, rinsed carefully in distilled, deionised water and dried on a solid piece of teflon. To minimise cracking during drying, the rate of drying was retarded by sealing the film in a container with various saturated salt solutions. In this manner, the humidity was stepped down from 94% to about 50% over a period of 5 days. Once dried, films were approximately 300  $\mu\text{m}$  thick.

### Synthetic Melanin Powders

Synthetic powders of DOPA-melanin were extracted from the black, electropolymerised dl-DOPA solutions by acidification to pH 2.0 with 6 M hydrochloric acid. The precipitated melanin was separated from the solution by centrifugation at 3500 rpm for 10 minutes, rinsed and then dried in air. Powders were pressed at 400 MPa into pellets 0.4 to 1.0 mm thick as recommended by the ASTM ‘standard test methods for measuring resistivity and hall coefficient and determining hall mobility in single-crystal semiconductors’ [29]. Pellets were 1.27 cm in diameter.

### Sample Contacting

Gold contacts were applied to the samples by thermal evaporation and copper wires attached to the gold with silver paint or conductive epoxy. Prior to contacting, samples were glued onto a glass slide with araldite for support.

For conductivity measurements, contacts to the samples were made in the van der Pauw configuration [31] as seen in figure 4.1. According to van der Pauw, the contacts should be very small. However, this was not possible as the G $\Omega$  resistance of the sample meant that correct placement of the contacts would produce currents too small to be measured. The uncertainty introduced by large contacts was calculated from the expressions given by van der Pauw. This analysis will be detailed in the next section 4.2.

The van der Pauw configuration was chosen over a the two-electrode sandwich configuration used by Jastrzebska *et al.* [1] as it leaves a much greater surface area exposed for maximal water vapour adsorption. Additionally, as it is a four point method, it eliminates the effect of contact resistance.[30] It was chosen over a linear four-point arrangement as the simple cross mask required for the van der Pauw configuration is much simpler to construct. Attaching the copper wires is also easier in the van der Pauw configuration than in a linear arrangement.

#### 4.1.2 Measuring Conductivity at Various Relative Humidities

Conductivities were measured using the van der Pauw technique [31] detailed in the National Institute of Standards and Technology *Hall Effect Measurements* procedure

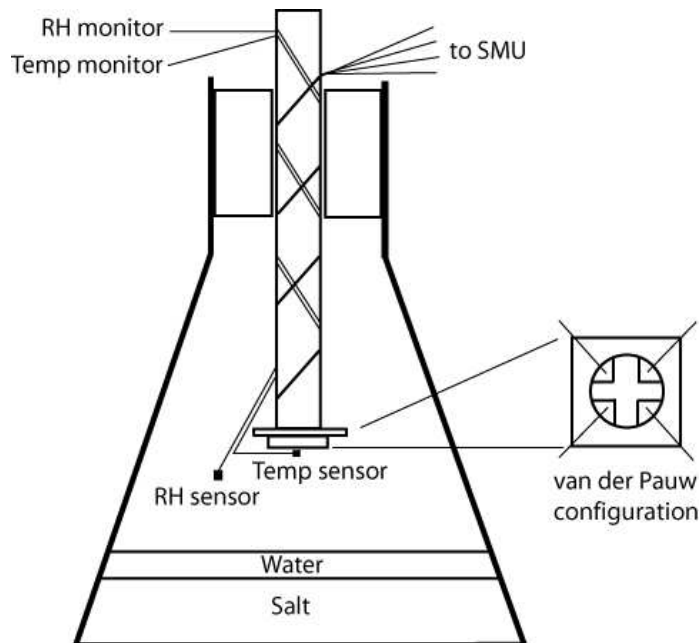


**Figure 4.1:** Experimental setup for measuring the conductivity of a melanin sample at various relative humidities. The saturated salt solution in the bottom of the sealed flask controlled the relative humidity. A hygrometer monitored the relative humidity (RH). Voltage was applied across the sample and current measured using a source-meter unit (SMU).

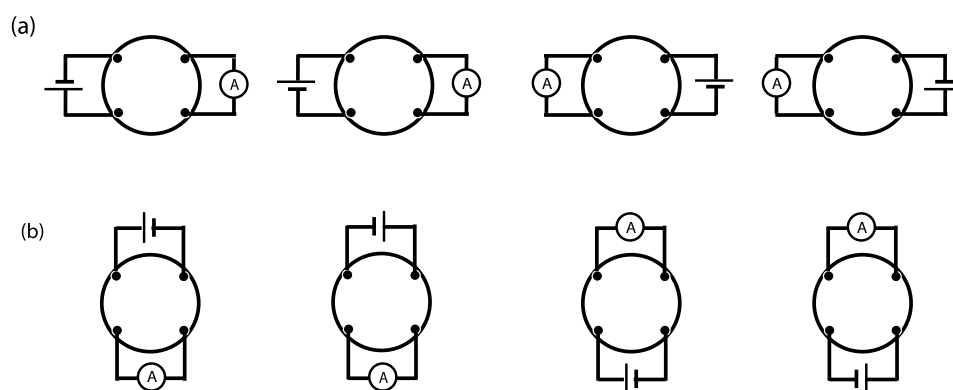


**Figure 4.2:** The eight different (a) ‘vertical’ and (b) ‘horizontal’ configurations of electrodes from which current-voltage curves were obtained in order to calculate the conductivity of the sample according to the van der Pauw method [31].

[32].

Current-voltage (IV) curves were measured using a Keithley 2400 Source Meter Unit (SMU) over the approximate range 0 to 5 V in 0.5 V increments with a settling time of 0.5 s. In cases where the ohmic region of the IV curves was quite narrow, an additional scan over the ohmic range with 0.1 V increments was performed. It should be noted that usually the van der Pauw method requires current to be applied and voltage to be measured. However, the mode of operation of the SMU allowed us to specify the voltage and input a current required to give the specified voltage.

In accordance with the NIST procedure, eight IV curves were obtained for each conductivity measurement at each different relative humidity. Four curves corresponded to the four different ways of applying a voltage across two contacts and measuring the current through the other two contacts with electrodes in the ‘vertical’ configuration seen in figure 4.2(a). The remaining four curves were measured with electrodes in the ‘horizontal’ configuration seen in figure 4.2(b). A resistance  $R_A$  was calculated from the slope of the first four IV curves and a resistance  $R_B$  from the second four. The conductivity  $\sigma$  of the sample was then calculated from the van der Pauw equation

$$\exp(-\pi R_A d \sigma) + \exp(-\pi R_B d \sigma) = 1 \quad (4.1)$$

where  $d$  is the thickness of the sample. The iterative algorithm in the NIST procedure was used to solve this equation for  $\sigma$ .

Hydration of the samples was controlled by placing various saturated salt solutions in a sealed conical flask with the sample as seen in figure 4.1, in accordance with the ASTM ‘standard practice for maintaining constant relative humidity by means of aqueous solutions’ [33]. The system was allowed to equilibrate for at least sixteen hours before making measurements. Additional salts at desired humidity levels were selected from Greenspan [34]. The relative humidity in close proximity to the sample was monitored with a Sper Scientific 800039 hygro-thermometer. IV Measurements were made only when the relative humidity was within 5% of its theoretical value. The temperature at close proximity to the sample was also monitored throughout the measurements using a thermocouple.

Nominally zero percent relative humidity measurements were performed under a vacuum applied by a rotary pump. The level of vacuum was not measured. Instead, the resistance of the sample as the flask was pumped down was monitored. As expected, the resistance increased as the vacuum became stronger. The vacuum deemed to be strong enough when the resistance reached a steady state. In all cases this occurred after approximately 10 minutes.

The conical flask was wrapped completely in aluminium foil to eliminate any photoconductive effects.

Measurements were performed on two pellets of pressed melanin powder of thickness 950  $\mu\text{m}$  and 560  $\mu\text{m}$  and one 290  $\mu\text{m}$  thick electropolymerised melanin film.

## 4.2 Results

Figure 4.3 shows a representative sample of the IV plots obtained at various relative humidities. As can be seen, for the curves at 11% and 23%, there is a significant departure from ohmic behaviour at 0.2 and 3.5 V respectively. At 74% and 81% higher humidities there is a small departure from ohmic behaviour at about 4.5 V. For these curves, only data in the ohmic range was used in the conductivity calculations. All other curves were ohmic over the 0 to 5 V range.

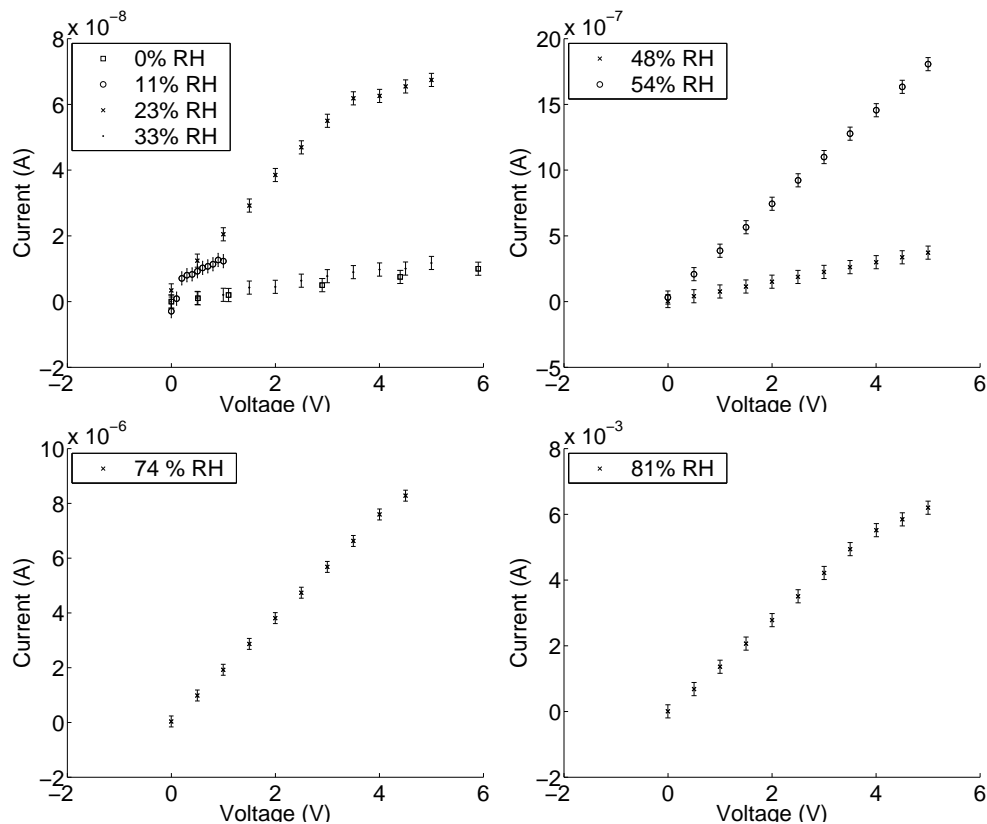


**Figure 4.3:** Representative sample of current-voltage curves of melanin at various hydrations. These curves were measured on the  $560\ \mu\text{m}$  pellet. Notice the departure from ohmic behaviour at 11% and 23% relative humidity (top left panel). The reason behind this departure will be explored in chapter 7. Also note the change in y-axis scale between the plots.

Figure 4.4 shows how the conductivity of the melanin samples varied with relative humidity at  $(24 \pm 2)^\circ\text{C}$ . As stated in section 4.1.1, the main source of the uncertainty in the conductivities was that introduced by having larger than ideal contact areas. According to van der Pauw [31], the relative uncertainty in the con-

ductivity introduced by having a contact span a distance  $l$  of the circumference of a disk of diameter  $d$  is

$$\frac{\Delta\sigma}{\sigma} = \frac{l^2}{16d^2 \ln 2}. \quad (4.2)$$

For our contacts on one of our pellets this equates to

$$\frac{\Delta\sigma}{\sigma} = \frac{7.65^2 \text{mm}^2}{16 \times 12.7^2 \text{mm}^2 \times \ln 2} \quad (4.3)$$

$$= 3.3\%. \quad (4.4)$$

The additional uncertainty introduced by having a contact intrude perpendicularly a distance  $m$  from the circumference into the pellet is

$$\frac{\Delta\sigma}{\sigma} = \frac{m^2}{4d^2 \ln 2}. \quad (4.5)$$

Using this equation, the maximum uncertainty introduced into our measurements from this cause is

$$\frac{\Delta\sigma}{\sigma} = \frac{4.71^2 \text{mm}^2}{4 \times 12.7^2 \text{mm}^2 \times \ln 2} \quad (4.6)$$

$$= 5.0\%. \quad (4.7)$$

Assuming that the two ways in which errors are introduced are independent, the total error per contact is  $\sqrt{3.3^2 + 5.0^2} = 6\%$ . According to van der Pauw, the total error introduced by having four non-ideal contacts is, to a first approximation, simply the sum of the errors per contact. This gives a total uncertainty of 24%. We assumed that the uncertainty due to large contacts on the film is the same as that for the pellets.

Since the relative humidity is not directly proportional to the amount of water absorbed by the melanin, to obtain more meaningful information from figure 4.4, we must convert the x-axis from relative humidity to weight percent water. The relationship between relative humidity and weight percent water is given by the adsorption isotherm of melanin. We used the isotherm from Powell and Rosenberg [25] seen in figure 4.5.

Figure 4.6 shows the relationship between the conductivity of the three melanin samples and the weight percent of absorbed water. The conductivity of all three samples show the same qualitative behaviour: it increases as the weight percent of absorbed water increases from 0% to approximately 10%, it then decreases by about one order of magnitude between about 10% and 15% until at 15% it suddenly increases sharply again. Overall, the conductivity increases 6 to 7 orders of magnitude from about  $10^{-9}$  S/cm to about  $10^{-2}$  S/cm as the weight of adsorbed water increase from 0% to about 27%. The similarities in the behaviours of the pressed powders and the film is somewhat surprising because we thought the structure of

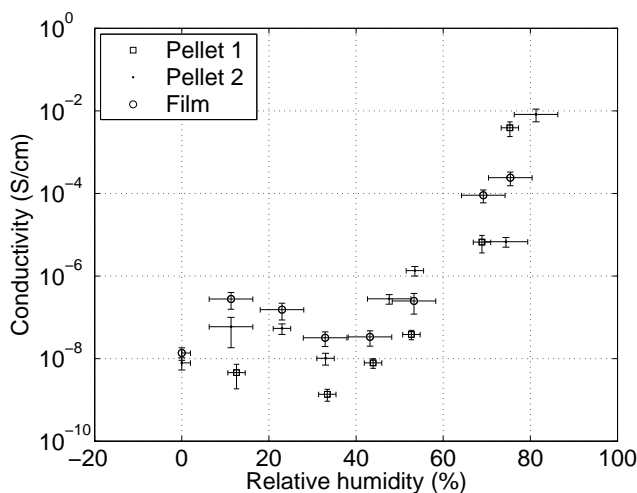


**Figure 4.4:** Conductivity of solid state synthetic melanin as a function of relative humidity at  $(24\pm 2)^\circ\text{C}$ . Pellet 1 was  $950\ \mu\text{m}$  thick, pellet 2 was  $560\ \mu\text{m}$  thick and the electropolymerised film was  $290\ \mu\text{m}$  thick. All three samples show similar behaviour.

the film would be quite different to the structure of the pellets at the microscopic level, resulting in different hydration-dependent conductivities.

Comparing the results displayed in figure 4.4 with those of the experiment by Jastrzebska *et al.* [1] seen in figure 2.6, we see the results are similar in some regards and different in others. Both show the lowest conductivity occurs under vacuum and both appear to show an exponential relationship between the conductivity and relative humidity in the 40 to 100% humidity range. The vacuum conductivity measured by Jastrzebska *et al.* is likely to be more representative of the true vacuum conductivity than our measurement which is several orders of magnitude higher, as their measurements were performed with an electrometer, which can more accurately measure small currents.

The major differences between the two sets of data is the overall order of magnitude of the conductivity and the absence of the dip in conductivity in their data. In their experiment, Jastrzebska *et al.* used a sandwich electrode configuration on similarly sized samples to us, but waited only one hour to obtain hydration equilibrium. As the sandwich configuration leaves very little surface area exposed and the equilibration time was short, it is likely that the bulk of the sample was at a hydration level lower than equilibrium, resulting in the lower measured conductivities. In regards to the lack of a dip in the conductivity measured by Jastrzebska *et al.*, no measurements were made by them in the 10 to 35% relative humidity range where we observed the dip. This region appears very important, as we shall see later.

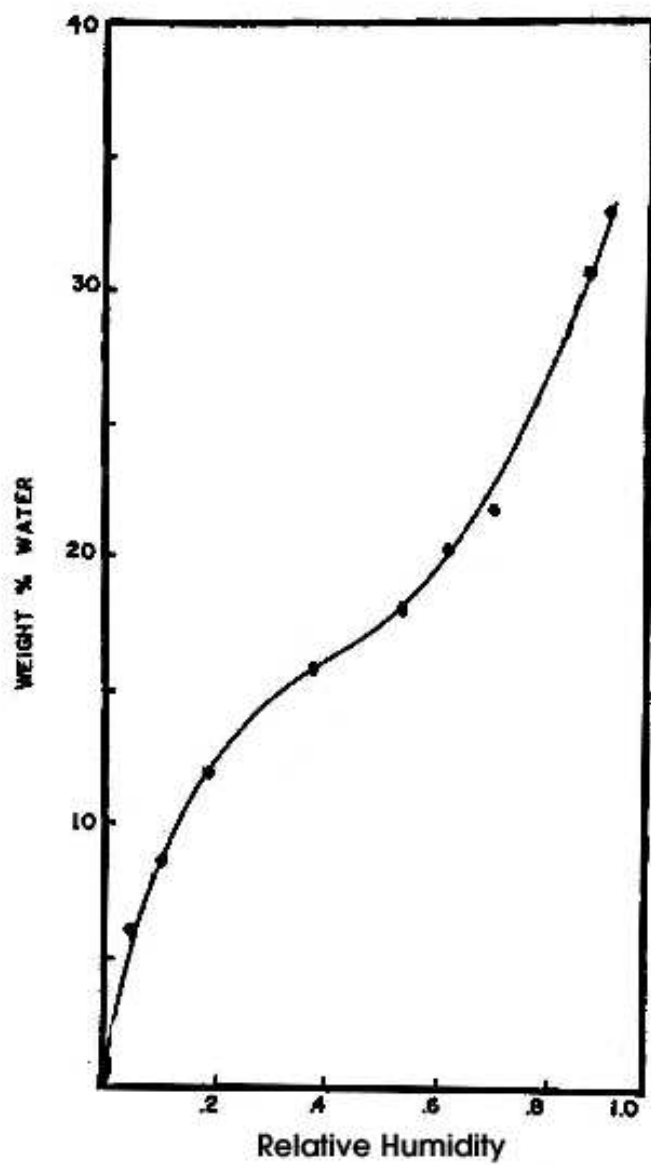


**Figure 4.5:** Water adsorption isotherm for synthetic melanin powder. Melanin produced by auto-oxidation of DOPA. Taken from [25]. Note that relative humidity is expressed as a decimal rather than a percentage.

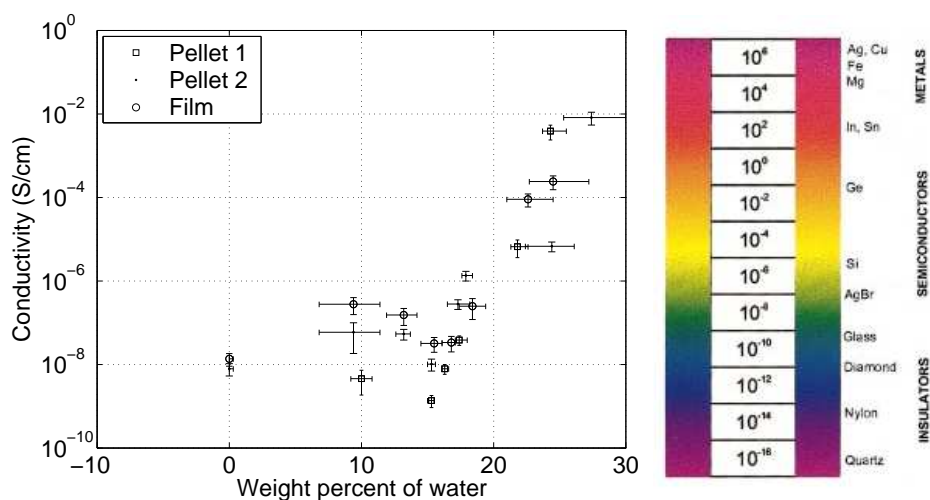


**Figure 4.6:** Conductivity of solid state synthetic melanin as a function of weight percent of adsorbed water. Pellet 1 was  $950 \mu\text{m}$  thick, pellet 2 was  $560 \mu\text{m}$  thick and the electropolymerised film was  $290 \mu\text{m}$  thick. The table on the left shows the conductivities of some common materials for comparison. All three samples show similar behaviour.

### 4.3 Discussion

The repeatable departure from ohmic behaviour at 11% and 23% relative humidity in figure 4.3 was an unexpected feature which is difficult to explain in the framework of electronic conduction. When this behaviour was first observed, our immediate reaction was that the contacts were non-ohmic. However, non-ohmic contacts usually cause a Schottky diode type IV curve. This is the opposite effect to the saturation of the current which we observe. Additionally, if the contacts were non-ohmic then we would expect to see similar behaviour at all humidities. We will come back to possible reasons for this behaviour in chapter 7.

To explain the results in figure 4.6, we considered in turn the two theories of how water affects the conductivity of melanin presented in chapter 3. Examining the percolation equation 3.2 and the Rosenberg equation 3.10, we see that neither alone can explain the observed relationship between the conductivity of melanin and the weight percent of adsorbed water. However, the two theories do qualitatively fit certain regions of the data. The Rosenberg equation predicts a plateau in the conductivity, which we see at around 10 to 15 wt% water. Meanwhile, percolation theory predicts a sudden increase in the conductivity according to a power law when the percolation threshold is reached. We see a sudden increase in the conductivity at around 15 wt% water.

To fit the Rosenberg equation to the conductivity data between 0 and 15 wt%

adsorbed water, we must first derive a relationship between the hydrated dielectric constant  $\kappa_w$  and weight percent water  $w$ . This function has three requirements:  $\kappa_w = \kappa$  at 0 wt% water,  $\kappa_w$  increases as  $w$  increases, and  $\kappa_w$  tends to 80 (the dielectric constant of water) as  $w$  tends to infinity. The simplest function that satisfies these requirements is

$$\kappa_w = \frac{80w + \kappa}{w + 1} \quad (4.8)$$

as can be seen in figure 4.7. In this figure, the dielectric constant of the dry macromolecule  $\kappa$  is set to 50. This value was the real part of the complex dielectric permittivity of melanin at low frequency measured in [35].

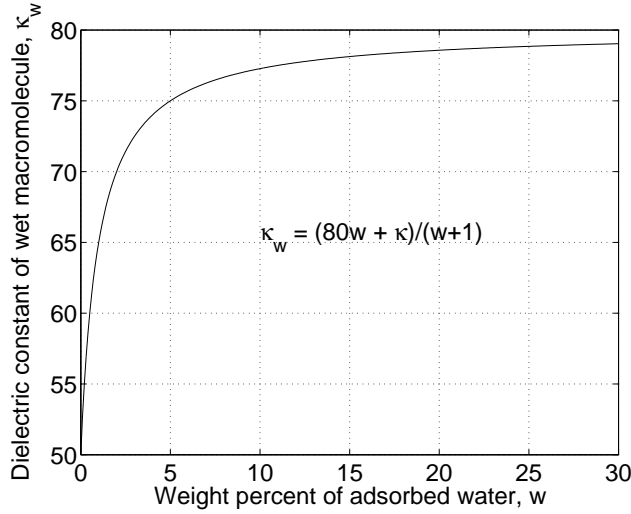


**Figure 4.7:** Proposed relationship between the dielectric constant of a wet biomacromolecule  $\kappa_w$  and the weight percent of absorbed water  $w$ . The dielectric constant of the dry biomacromolecule  $\kappa$  is set to 50.

Substituting this function into the Rosenberg equation 3.10 and rearranging gives

$$\sigma = \sigma_0 \exp \left[ \frac{-E_D}{kT} \right] \exp \left[ \frac{q^2}{4\pi\epsilon_0 kTR} \left( \frac{1}{\kappa} - \frac{w+1}{80w+\kappa} \right) \right] \quad (4.9)$$

$$= \sigma_0 \exp \left( \frac{-E_D}{kT} \right) \exp \left( \frac{q^2}{4\pi\epsilon_0 kTR\kappa} \right) \exp \left( -\frac{q^2}{4\pi\epsilon_0 kTR} \frac{w+1}{80w+\kappa} \right) \quad (4.10)$$

$$= A \exp \left( -B \frac{w+1}{80w+\kappa} \right). \quad (4.11)$$

Hence, A and B are positive constants which can be found from the slope and intercept of a plot of  $\ln(\sigma)$  against  $(w+1)/(80w+\kappa)$  for  $w$  between 0 and 15 wt%. This fit could only be performed for the 560 $\mu\text{m}$  pellet and the film as the 950 $\mu\text{m}$

pellet has only one measurement below 15 wt% water. The gradients and intercepts were found using linear regression. The fitted functions on a  $\log(\sigma)$  against wt% water are shown in figure 4.9. Note that there are really three free parameters in equation 4.11. As already stated, the variable  $\kappa$  was set to 50. However, trying alternative values showed that in fact, the appearance of the function in figure 4.9 was highly insensitive to the value of  $\kappa$ . Moreover, the appearance in figure 4.9 was highly insensitive to the form of the relationship between dielectric constant and adsorbed water all together. Even a linear relationship,  $\kappa_w \propto w$  gave a hydration-dependent conductivity which appeared very similar to that seen in figure 4.9.

The percolation equation 3.2 can be fitted to the conductivity data between 15 and 30 wt%. To do this, we assume that the weight percent water  $w$  is directly proportional to the probability  $p$  that a bond is intact or a site is occupied so that  $p = kw$  where  $k$  is a positive constant. We must also subtract the conductivity due to nonpercolative processes from the total conductivity as the conductivity in the percolation equation should be only that due to movement of charges along percolated pathways created by the adsorbate. With these modifications, equation 3.2 becomes

$$\sigma(w) - \sigma(w_c) = k^\mu(w - w_c)^\mu. \quad (4.12)$$

Hence a plot of  $\log[\sigma - \sigma(w_c)]$  against  $\log(w - w_c)$  should be linear with a slope of  $\mu$  and intercept of  $\mu \log k$ . But before we could fit this equation to our experimental data in this manner, the other free parameter—the critical weight percent water  $w_c$ —had to be chosen, and its dependent variable—the nonpercolative conductivity  $\sigma(w_c)$ —had to be calculated. The parameter  $w_c$  was chosen by optimising its value to give the smallest relative error in the slope  $\mu$ , calculated using linear regression. As the data above 15 wt% appeared fairly consistent between the three samples, the fit was performed considering the data from all three samples together above 15 wt% water. The optimal linear fit is shown in figure 4.8. Figure 4.9 shows the fitted function on a  $\log(\sigma)$  against wt% water plot.

The optimal fit of the percolation equation occurred with a percolation threshold of 10 wt% water. As the percolation threshold marks the onset of long-range connectivity, we expect that it should occur at approximately the adsorbed water level corresponding to a single layer (monolayer) coverage of melanin. Meanwhile, as stated in section 3.4, we expect that only water in the first monolayer will dramatically affect the dielectric constant, as only this layer of water can interact strongly with the melanin. The fit of the Rosenberg model seen in figure 4.9 predicts the electronic conductivity is saturated by 10 wt% water. Considering these two expectations, our analysis suggests that monolayer coverage of melanin occurs at around 10 wt% adsorbed water.

In the percolation analysis, the optimal critical exponent  $\mu$  was found to be  $11 \pm 1$ . This is obviously much higher than the theoretical critical exponents of 2D or 3D percolation (1.3 and 2.0 respectively). The reason for this discrepancy is not

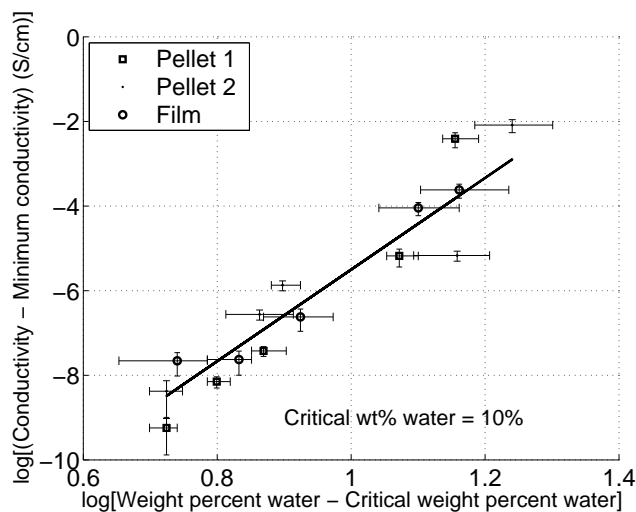


**Figure 4.8:** A log-log plot of the percolated conductivity of melanin as a function of the weight percent of absorbed water minus the weight percent of absorbed water at the percolation threshold. Optimal line of best fit was calculated using linear regression with uncertainty in the x-axis data as this uncertainty was much greater than that in the y-axis data.

known and its existence is a big blow for percolation theory. It could be that the assumption  $p = kw$  is incorrect. If we make some other assumption  $p = kw^\alpha$  we may get the correct critical exponent. However, a correct critical exponent requires  $\alpha$  to be 5-10 which is quite large. Really, more data is needed to give a better estimate of the percolation threshold and the conductivity at the percolation threshold. For now, the qualitative fit and the absence of alternative theories leads us to consider percolation theory further.

It should be noted that an exponential also provided a reasonable fit to the conductivity of melanin above 15 wt% water since over a small data range, a power and exponential look very similar. This analysis has not been included as no theory predicted such a relationship to exist between conductivity and hydration in this hydration range. To give a more definitive answer to the true dependence of the conductivity of melanin on hydration, more data is needed, particularly over a larger hydration range. Unfortunately, measurements at high hydration are very difficult as the samples become too soft to even maintain their shape.

#### 4.4 Proposed Conduction Mechanisms

Figure 4.9 shows us that at least qualitatively the observed dependence of the conductivity of melanin on hydration can be explained by the Rosenberg and percolation

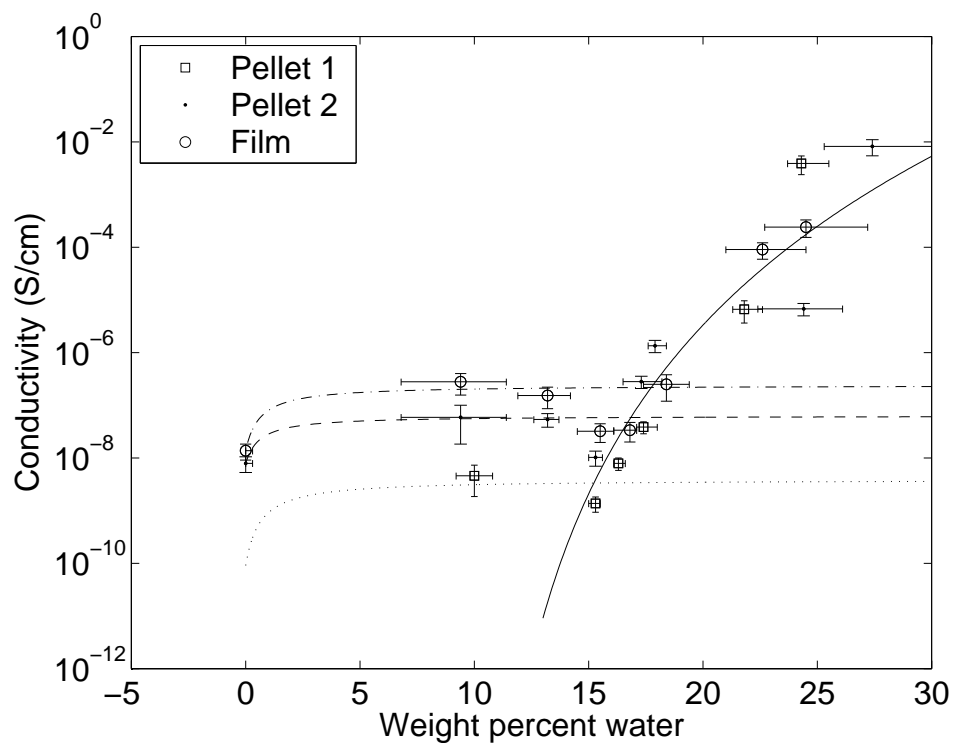


**Figure 4.9:** Fit of the Rosenberg (broken lines) and percolation (solid line) models to the conductivity of melanin as a function of weight percent of absorbed water. The Rosenberg model was fitted to data below 15 wt% water while the percolation model was fitted to data above 15 wt% water. Fit of the Rosenberg model to pellet 2 and the film are the dashed line and dash-dotted line respectively. The Rosenberg equation could not be fitted to the data from pellet 1 due to insufficient data below 15 wt% water. Hence, the dotted line was created by shifting the fit for pellet 2 down until it matched the pellet 1 data by eye.

models of how water affects conductivity.

Application of Rosenberg theory between 0 wt% and about 10 to 15 wt% adsorbed water implies that in this regime, the conductivity of melanin is predominantly electronic and changes with hydration due to the increase in effective dielectric constant of melanin as water is adsorbed.

Meanwhile, as already stated in section 3.5, application of percolation theory above 15 wt% hydration requires the additional water molecules to form either conducting bonds or conducting elements. If water is affecting *electronic* conduction in this regime then we require the water molecules to form electron-conducting bonds that connect electron-conducting islands of melanin. However, we have already seen in section 3.5 that this is not possible. Instead, to explain the qualitative fit between the observed conductivity and percolation theory, we require that as water is adsorbed onto melanin, it forms a hydrogen-bonded network in which protons can conduct.

The dip in the conductivity of melanin between 10 and 15 wt% water may be able to be explained in terms of some interaction between the two mechanisms before percolated conductivity dominates. We will explore this further in chapter 7. If this is the case, then we expect that the interaction would begin when the percolation threshold is passed. Since we begin to see a drop in conductivity as we pass 10 wt%, the proposed percolation threshold appears to be in agreement with observations.

## 4.5 Summary

In this chapter, we analysed the experimentally observed relationship between the conductivity and hydration of melanin. We showed that the observations could be explained qualitatively by applying the Rosenberg theory of how water affects conduction in the low hydration range, and applying percolation theory in the upper hydration range. However, the application of percolation theory requires protonic conduction. In the next few chapters, we will explore protonic conductivity; how it occurs, where it occurs, how we can observe it experimentally and its applicability to melanin. Armed with this information, we will then attempt to explain other features of the dependence of conductivity on hydration—the dip in conductivity between 10 and 15 wt% water—in chapter 7.

---

# Protonic Conduction

---

Protonic conduction is important in many biophysical processes such as photosynthesis.[36] It is also the main conduction mechanism in many organic and inorganic materials. Since we are examining the effects of hydration on melanin, this chapter focuses on protonic conductivity in hydrated systems. In this chapter, the types of hydrated systems and the basic mechanisms of protonic conduction in hydrated systems are outlined. Experimental signs that a material is a protonic conductor are described. Finally, protonic conduction in percolated systems is discussed as well as mixed conduction.

## 5.1 Mechanisms of Proton Conduction

Hydrogen ions  $H^+$  are bare protons. The absence of shielding electrons makes hydrogen ions highly reactive and as such, they do not exist independently in condensed matter.

In many materials, protons interact with solvent molecules such as water to form ‘classical’ ions such as hydroxide ions  $OH^-$  and hydronium ions  $H_3O^+$ .[37] Movement of these two species is technically a special case of ionic conduction, but can be thought of (and from here on will be referred to) as the vehicle mechanism of protonic conduction. This mechanism is essentially classical  $H_3O^+$  and  $OH^-$  ion diffusion as illustrated in figure 5.1(a). This special case of ionic conduction warrants separate consideration as water is the ubiquitous solvent, especially in biological systems.

The other main mechanism of conduction by protons is the Grotthus mechanism illustrated in figure 5.1(b). In this mechanism, protons are ‘relayed’ between hydrogen-bonded water molecules by tunnelling. Consequently, this mechanism of conduction is most efficient when a continuous hydrogen-bonded network exists, such as in ice. With the Grotthus mechanism, charge transport is significantly enhanced over the vehicle mechanism.[39, 40] It is generally accepted that the Grotthus mechanism prevails over the vehicle mechanism in most solid protonic conductors.[40]

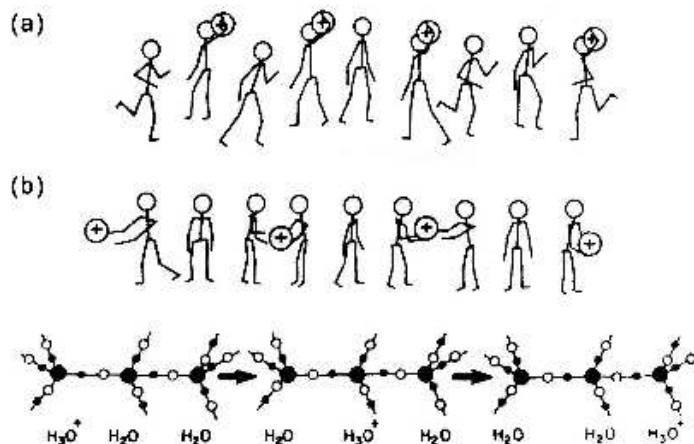


**Figure 5.1:** Pictorial representations of the (a) vehicle mechanism and (b) Grotthuss mechanism of proton conduction. In the example of the Grotthuss mechanism in a water chain, ● represents an oxygen, ● represents a filled proton position and ○ represents a potential but vacant proton position. Taken from [38].

## 5.2 The Effect of Water on Conductivity

As stated in chapter 3, water molecules are adsorbed onto the surfaces of materials exposed to water vapour. Water adsorption isotherms (such as melanin's seen in figure 4.5) are characteristic curves of the amount of water vapour adsorbed against the partial pressure of water vapour at constant temperature and pressure. There are five main types of adsorption isotherms.

Three of the adsorption isotherms correspond to a characteristic dependence of the conductivity on the partial pressure of water vapour.[37] These are illustrated in figure 5.2. Type (a) isotherms occur for intrinsic conductors. In materials of this type, water is adsorbed strongly at low concentrations and the amount of adsorbed water quickly saturates once monolayer coverage is completed. This results in the conductivity being relatively insensitive to water vapour partial pressure. Type (b) isotherms occur for systems where both intrinsic and surface conductivity must be taken into account while type (c) isotherms are typical of surface conductors. Both type (b) and (c) isotherms are usually characteristic of multilayer adsorption on non-porous solids.

In chapter 3 we already showed that a type (a) conductivity against water vapour partial pressure curve can be explained by water influencing intrinsic electronic conduction. In contrast, the type (b) and (c) isotherms in figure 5.2 do not correspond to particular conduction mechanisms. In fact, within a particular structure, the

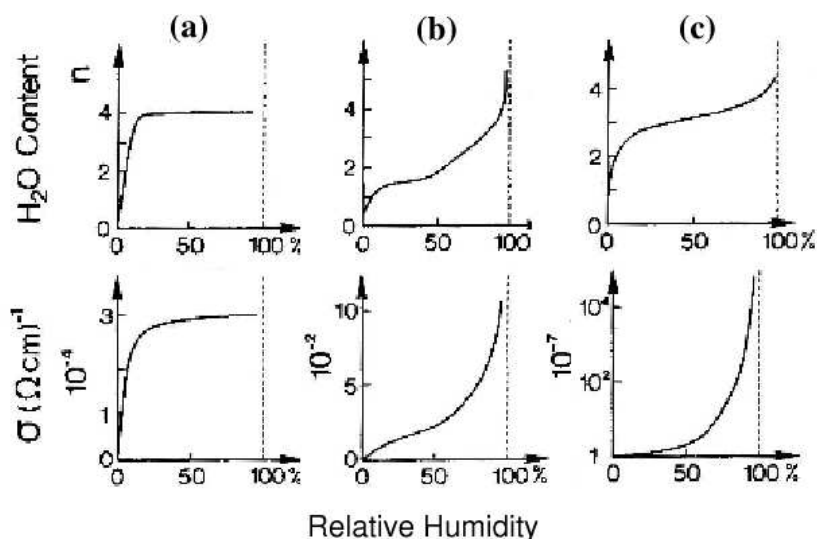


**Figure 5.2:** Influence of relative humidity on water content  $n$  and conductivity  $\sigma$  for (a) an intrinsic conductor, (b) a mixed surface-bulk conductor and (c) a surface conductor. Modified from a figure in [37].

conduction mechanism may change as a function of water vapour partial pressure and temperature.[37]

The discussion so far on protonic conduction in hydrated systems has not been reconciled with the fact that pure water is a very poor conductor. The poor conductivity is a result of a negligible density of free, mobile ions [40], as the only source of ions in pure water is the dissociation of water molecules;  $2\text{H}_2\text{O} \rightleftharpoons \text{OH}^- + \text{H}_3\text{O}^+$ . However, despite the low conductivity, the mobility of protons in pure water remains very high.[40] As a result, when an excess proton is donated to the water (however infrequently this may occur) it is transported very quickly.

It is the high mobility of protons in water that allows hydrates capable of donating or accepting protons to be good proton conductors. The most common sources of protons are ionisable groups such as acid groups. As water is adsorbed, these groups ionise to a degree determined by their  $\text{p}K_A$ , donating a high concentration of excess protons to the layers of adsorbed water and resulting in a high conductivity.

### 5.3 Protonic Conduction in Percolated Systems

An increase in the conductivity with adsorbed water can be due to a percolation process. As stated in chapter 3, percolation theory is not concerned with the mechanism of conduction, and so is as equally applicable to protonic conductors as electronic

conductors.[22]

In systems where conductivity increases with adsorbed water, the water molecules may act as conducting elements in site percolation. The percolation process is proton transfer along strings of hydrogen-bonded water molecules via the Grotthus mechanism. This can be the mechanism of surface conduction in types (b) and (c) isotherms in figure 5.2

An interesting consequence of percolated protonic conduction of this type is that the local structure of the conducting molecule becomes irrelevant. Instead, the water molecules acting as interconnected conducting elements are of primary importance.[41]

## 5.4 Experimental Evidence

Definitive proof of protonic conduction can be difficult to obtain due to alternative acceptable interpretations of many results in terms of processes not involving protonic conduction. Hence, it is generally accepted that a number of necessary but not sufficient criteria must be satisfied before a convincing case for protonic conduction can be made.[37, 38, 42]

Some of the criteria for protonic conduction are:

1. One of the most easily observed signs of protonic conduction is a decay in current with time under a constant applied voltage.[37, 42] This is caused by a build up of charge-carriers at the sample-electrode interface due to inefficient proton-electron exchange at the interface. This process is known as space-charge polarisation.
2. Another effect of space-charge polarisation is a transition from ohmic behaviour to a Child's law dependence of the current on the voltage ( $I \propto V^n$  where  $n \geq 2$ ) at sufficiently high applied voltages.[42]
3. Transference number measurements determine what percentage of the current passing through a sample is protonic.[37, 38, 42] In the coulometric method of measuring the transference number, a current is passed through the sample and the electrolysis products at the electrodes are collected and analysed. If conduction is protonic, oxygen and hydrogen are expected to evolve at the electrodes. The amount of oxygen and hydrogen can be compared to the theoretical yield calculated from Faraday's law of electrolysis, assuming 100% ionic conduction. Differences between the theoretical and actual yields reveal the percentage of the current carried by protons and the percentage carried by electrons.
4. In semiconductor physics, Hall effect measurements are a commonly used method of determining the sign of the majority charge carrier. If protonic

---

conduction is the dominant conduction process in a material, then the Hall voltage should be positive.[37, 42]

5. Thermoelectric effect measurements should also show that the majority charge carriers are positive.[42]
6. Nuclear magnetic resonance (NMR) can be used to examine the dynamics of protons in suspected protonic conductors. ‘Line narrowing’ on a NMR spectrum of a solid occurs when a proton is exchangeable and free to move.[38]
7. Inelastic scattering of slow neutrons is another useful method of studying proton dynamics.[38, 42]. The energy gain or loss in the material after neutron scattering provides information on the energy levels of the hydrogen bonded systems in the material.[42]

## 5.5 Mixed Conductors

It is worth noting that materials can be mixed protonic and electronic conductors and the proportion of current carried by either mechanism may change as a function of temperature and/or hydration. In fact, most biopolymers subject to conduction studies have been found to be mixed conductors. This will be further discussed in the next chapter.

For biopolymers, the likelihood of mixed conduction makes determining the conduction mechanism particularly challenging. Proving protonic conduction is difficult, but determining under which conditions either conduction mechanism dominates in a mixed conductor is even more challenging as the problem of alternative interpretations of experimental results is exacerbated.

## 5.6 Summary

This chapter has outlined the mechanisms of protonic conduction in hydrated systems and the experimental signs of a protonic conductor. In chapters 6 and 7 we will explore the relevancy of these concepts to melanin and other biopolymers.



---

# Charge Transport in Biological Macromolecules

---

Compared to melanin, the debate on charge transport mechanisms in other biological macromolecules like proteins has been more intense and focused. Like melanin, the presence or absence of water appears to play a significant role in the conduction properties of all these systems [1, 43], in accordance with the existence of these molecules *in vivo* in aqueous environments. It should be noted that we are only discussing conduction mechanisms in the bulk condensed phase not along single molecules.

For proteins, the main debate about charge transport centres on whether the conduction mechanism is protonic or electronic.[25] As we have already seen in chapters 3 and 5, the significant effect of water on the physical properties of biomolecules may occur with either of the two mechanisms. Water can alter the conductivity by modifying the dielectric constant causing a change in the activation energy for conduction by electrons, or it can provide a network that greatly increases the mobility of protons, enhancing protonic conduction.

This chapter briefly reviews the debates on charge transport mechanisms in the proteins collagen and lysozyme as examples of the current thinking about charge transport in biological macromolecules. Other experiments on melanins are then described and a case for partial protonic conduction in melanin is presented.

## 6.1 Collagen

For the protein collagen, an emphasis has been placed on interpreting the results of studies on the effects of hydration in terms of different charge transport mechanisms. A study of the conductivity of collagen at different hydration levels revealed an exponential dependence of the conductivity on hydration.[43] Conductivity increased from  $\sim 10^{-15}$  to  $10^{-9}$  S/cm when the weight percent of water was increased from  $\sim 1\%$  to  $23\%$  at  $23^\circ\text{C}$ .

Another detailed study of the conductivity of collagen as a function of water

content and temperature also found that conductivity increased with water content and temperature.[44] In this study, a lack of time dependency of the current and Ohmic behaviour at water contents below 20% relative humidity was interpreted as an indicator of electronic conduction. At higher humidities, currents were observed to be time dependent suggesting protonic conduction. It was also suggested that a change in the dependence of the activation energy on humidity at about 45% relative humidity could be due to increased proton mobility. Though it was not proposed, this could be due to the formation of a percolation pathway at this point. It may be that strongly bound water affects the dielectric constant, while all water participates in percolated protonic conduction. The presence of two types of water in collagen, a strongly bound and a weakly bound fraction, is supported by dielectric measurements.[45]

Direct evidence for protonic conduction is given by coulometric measurements by Powell and Rosenberg [25] who found that hydrogen gas was evolved during electrolysis at all hydration levels. They found that for humidities higher than  $\sim 30\%$ , at least 70% of the current is carried by protons.

In general, all studies of collagen found it to be a mixed semiconductor.

## 6.2 Lysozyme

Like collagen, experimental studies on the conductivity of the protein lysozyme have also suggested that the dominant charge carriers may be electrons in dry lysozyme and protons in hydrated lysozyme.[46].

Moreover, the conductivity of lysozyme has been explored in the framework of protonic percolation discussed in section 5.3 in several studies [41, 47]. As seen in figure 6.1, the DC conductivity of lysozyme was found to vary with hydration according to the percolation equation 3.2.[47] Interestingly, calculated critical exponents of 1.3 at low hydration changing to 2.0 at high hydration are in exact agreement with the theoretical values for two dimensional and three dimensional percolation. In this study it was assumed that the percolation probability was directly proportional to the weight percent of adsorbed water.

## 6.3 Melanin

### 6.3.1 The Story So Far

Chapter 2 has already discussed many studies on the solid state properties of melanin which relate to the charge transport mechanism. We have already seen that none of these studies assist significantly in determining how charge is transported or even the nature of the charge carrier in melanin.

Chapter 4 showed the results of our experiment on conductivity of melanin with hydration control fitted semi-quantitatively with the theory of how water can affect

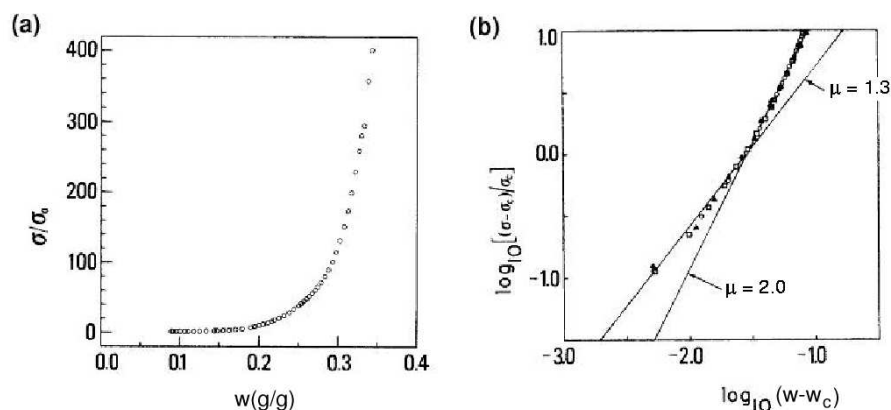


**Figure 6.1:** The DC conductivity of lysozyme powder as a function of hydration. (a) The normalised DC conductivity  $\sigma/\sigma_0$  against weight fraction of adsorbed water  $w$  on a linear plot. (b) A log-log plot of the conductivity as a function of  $w$  minus the weight percent of adsorbed water at the percolation threshold  $w_c$ . The slope of this plot is the critical exponent of percolation  $\mu$ . Modified from a figure in [47].

electronic conduction in amorphous semiconductors and with percolation theory. However, as discussed in section 3.5 an explanation in terms of percolation theory required water molecules to be conducting elements which is not consistent with conduction by electrons. Chapter 5 showed us that water molecules *can* be conducting elements in a site percolation picture if *protons* are the charge carriers. This suggested that protonic conduction in melanin warranted investigation. This investigation is supported by studies on proteins, outlined in this chapter, which concluded that conductivity in proteins is partly due to the movement of protons.

### 6.3.2 A Case for Protonic Conduction in Melanin

Superficially, simply comparing the adsorption isotherm of melanin in figure 4.5 with the possible isotherms in figure 5.2, suggests that melanin may be a mixed intrinsic and surface conductor. And we have already seen in section 5.3 that surface conduction can be protonic, especially in hydrated conductors.

Re-examining the literature on melanin, we found that several studies have results consistent with the signs of a protonic conductor outlined in section 5.4.

A coulometric study by Rosenberg and Powell [25] found that 65% of current in synthetic melanin was attributed to protons and the remaining 35% to electrons. This did not change as a function of the hydration level over a hydration range of 12 to 35 wt% water. Hence, Rosenberg and Powell concluded that protons are the majority charge carriers in this hydration range. However, they did not observe a jump

in the charge carrier ratios as might be expected if the adsorbed water molecules suddenly formed a continuous percolated pathway at some critical hydration level.

Hall voltage measurements on natural melanin samples by Trukhan, Perevozchikov and Ostrovskii were positive, indicating a positive charge carrier.[17] Unfortunately, the hydration level of the sample during these measurements was not recorded. However, it is likely to have been at room temperature and pressure which corresponds to a relative humidity of  $\sim 40\%$ . In this paper, it was suggested that the charge carriers were holes. However, it was acknowledged that an equally valid interpretation of these results could be made in terms of melanin being a proton conductor.

Two studies of the thermoelectric effect in melanin suggest different dominant charge carriers at different hydrations. Measurements under vacuum [49] and after water loss by heating [48] gave a negative thermoelectric voltage suggesting negative charge carriers at low hydrations. Meanwhile, measurements of a positive thermoelectric voltage at ambient hydration [48] suggested positive charge carriers.

In their study on the electrical properties of synthetic melanins under vacuum, Osak *et al.* also observed a change from an ohmic to a Child's law dependence of the current on the applied voltage for high fields. As mentioned in section 5.4, this is one of the indicators of protonic conduction. Another sign of protonic conduction—a decay in current when a field is applied—was also observed in this study. Owing to the negative thermoelectric voltage, Osak and his colleagues attempt to explain their other observations in terms of electronic conduction. They propose that increasing the temperature induces conformational changes in melanin that allow electron hopping to occur more frequently, thus increasing the conductivity.

The conductivities observed in the study by Osak *et al.* ranged between about  $10^{-14}$  and  $10^{-12}$  S/cm, in accordance with the vacuum conductivity observed by Jastrzebska *et al.* [1]. In both studies, this intrinsic conductivity was attributed to electrons. However, it is several orders of magnitude below the conductivity of hydrated melanin. The increase in conductivity with absorbed water was not considered by Osak *et al.*.

The Child's law and current decay results can be explained most naturally by a protonic conduction mechanism. Under vacuum, we expect that all the free water is removed but it is possible that the bound water is only partially removed.[1] In this situation, the majority charge carriers would be electrons but the residual water molecules could give a minority protonic component to the conductivity via the vehicle mechanism. The thermoelectric effect tells us the sign of the dominant charge carriers (the electrons), while the observations of a Child's law dependence and decreasing current with time show us that protons are still present and conducting. This interpretation is supported by the observation that the current dropped very slowly with time, taking  $10^3$  to  $10^5$  seconds to reach steady state. As the water molecules are tightly bound, the frequency of hopping between binding sites is very low causing the extremely slow decay.

---

According to the criteria for protonic conduction outlined in section 5.4, five out of the seven criteria appear to be satisfied by melanin. Experiments examining the two remaining criteria—NMR line-narrowing and slow neutron scattering—have not been performed to date. For this reason, it is possible that charge conduction in melanin occurs at least partly by protonic mechanisms. More specifically, we propose that melanin is a mixed conductor, with majority electronic conduction at low hydration levels and a majority protonic conductor at high hydration levels. In addition to the evidence from the literature already presented, we shall also show in the next chapter that the significant departure from ohmic behaviour in the IV curves at 11% and 23% relative humidity seen in figure 4.3 supports the existence of protonic conduction in melanin.

## 6.4 Summary

The similarities between results of solid state studies on melanin and several proteins suggests that charge transport in these systems may be similar (although melanins are much more electrically active and photoconductive). This alone implies that the charge transport mechanism in melanin may be both protonic and electronic, with the relative contributions depending on the hydration level. Several other studies on melanin give more direct evidence that the conduction mechanism in melanin is protonic under some conditions.

These similarities between the results for the different biological macromolecules is quite surprising as the systems bear few structural similarities. This fact suggests that the conduction mechanism is at most only partially dependent on the primary structure of the macromolecule. We have already seen in section 5.3 that this independence of local structure is possible if percolated protonic conduction in a water molecule network is the mechanism of conduction.



---

# Re-examining the Effect of Adsorbed Water on Conductivity

---

We have now seen that a substantial case for protonic conduction in melanin can be made from the results in the literature. In this chapter, we re-examine the dependence of the conductivity of melanin on hydration which we presented in chapter 4, in light of the theory and literature on protonic conduction presented in chapter 5 and 6.

## 7.1 Proposed Conduction Mechanisms Revisited

Backed by the experimental evidence supporting protonic conduction in hydrated melanin, we propose that protonic conduction occurs in the percolated regime identified in chapter 4 above 10 wt% water. Similar to the conduction mechanism in lysozyme discussed in chapter 6, protonic conduction in the percolated regime in melanin may occur via the Grotthuss mechanism of proton transfer along threads of hydrogen bonded water molecules. The excess protons for conduction could be provided by the many ionisable groups of the DHI, DHICA and precursors molecules which make up melanin as seen in figure 7.1.

A simple order of magnitude calculation demonstrates that the number of protons required to give the observed conductivities could feasibly be provided by ionisation reactions of this type. The number density of protons  $N_P$  required to give the observed conductivities  $\sigma$  can be calculated from the relation

$$N_P = \frac{\sigma}{q\mu} \quad (7.1)$$

where  $q$  is the charge on the proton and  $\mu$  is the mobility of a proton. The proton densities required to give the observed conductivities as calculated using this relation are summarised in table 7.1. In this calculation, the mobility of the proton was

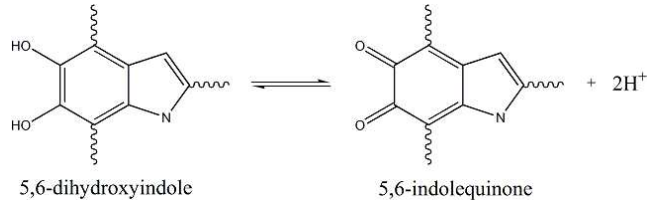


**Figure 7.1:** Example of the ionisation of a DHI or DHICA monomer molecule to give excess protons which may conduct.

assumed to be  $3.62 \times 10^{-3} \text{ cm}^2/(\text{Vs})$ , the proton mobility in water.[50]

The number density of monomers  $N_M$  in the system can be estimated if we assume that melanin is made of 50% DHI and 50% DHICA. Assuming all protons are attached, the molar mass of DHI is 149 g/mol and molar mass of DHICA is 181 g/mol giving an average molar mass  $MM$  of 165 g/mol. The number density of monomers is then

$$N_M = \frac{\text{Mass of sample}}{MM} \times \frac{\text{Avogadro's number}}{\text{Volume of sample}} \quad (7.2)$$

$$= \frac{\text{Sample density} \times \text{Avogadro's number}}{MM}. \quad (7.3)$$

Sample masses ranged from 0.01 g to 0.1 g and corresponding sample volumes were estimated from the geometries of samples to be  $5 \times 10^{-3} \text{ cm}^3$  to  $5 \times 10^{-2} \text{ cm}^3$ . This equates to a sample density of  $2 \text{ g/cm}^3$ . Substituting this value and the average molar mass into equation 7.3 gives a monomer density of approximately  $7 \times 10^{21}$  monomers/ $\text{cm}^3$ . With this number, the number of protons per monomer required to give the observed conductivities can be calculated using

$$\text{Number of protons per monomer} = \frac{N_P}{N_M}. \quad (7.4)$$

The number of protons per monomer estimated in this way for the various observed conductivities are summarised in table 7.1. Considering dissociation reactions such as that illustrated in figure 7.1 lie quite far to the left with excess water, and in the solid state the monomers are not necessarily in an excess water environment, the order of magnitude estimates of number of protons per monomer seems quite reasonable.

Since a static, very well-ordered water network can only exist below  $0^\circ\text{C}$ , the disagreement with the theoretical critical exponent of percolation may be due to the complication of elevated temperature. We expect that at room temperature, the hydrogen bonds connecting water molecules to each other and melanin would be weaker and would fluctuate. This could allow proton conduction via a combination

Conductivity (S/cm)	Required number density of protons (cm <sup>3</sup> )	Required number of protons per monomer
10 <sup>-2</sup>	1.7 × 10 <sup>19</sup>	10 <sup>-3</sup>
10 <sup>-4</sup>	1.7 × 10 <sup>17</sup>	10 <sup>-5</sup>
10 <sup>-6</sup>	1.7 × 10 <sup>15</sup>	10 <sup>-7</sup>
10 <sup>-8</sup>	1.7 × 10 <sup>13</sup>	10 <sup>-9</sup>
10 <sup>-10</sup>	1.7 × 10 <sup>11</sup>	10 <sup>-11</sup>

**Table 7.1:** Order of magnitude estimates of the number of protons required per monomer to give the observed conductivities.

of vehicle and Grotthus mechanisms. Free protons could conduct via the vehicle mechanism until they encountered a cluster of water molecules. The proton could then separate from its vehicle H<sub>2</sub>O and conduct through the cluster via the Grotthus mechanism. In this way, protons would be transported quickly through water clusters and more slowly through the gaps between clusters. The ability of protons to traverse gaps in the percolated network would lead to a larger conductivity than that resulting from percolated processes alone.

Furthermore, with a proton current, the departure from ohmic behaviour in the IV curves at 11% and 23% relative humidity seen in figure 4.3 can be explained. It could occur due to either a combination of a deficit of protons as charge carriers or a space-charge polarisation effect. Just past the percolation threshold, we expect that many protons will get trapped in dead-end hydrogen-bonded water threads and will not reach the negative electrode within the measurement time. Also, any protons that reach the negative electrode cannot be quickly transported away by water molecules, as there are not many water molecules in the system. At higher humidities, many hydrogen-bonded water threads span the entire sample and the system may begin to behave more like a gel than a solid. This is evidenced by the fact that at a relative humidity of 90%, no measurements were possible as the samples no longer even maintained their shape. Like liquids, gels are able to dissipate internal fields by molecular rearrangement. Hence, at higher humidities, we see a dramatically decreased or no departure from ohmic behaviour because more protons are able to move between electrodes entirely via the fast Grotthus mechanism, and there is enough water in the system to dissipate the space-charge field. We note that saturated IV curves are another experimental observation which can be explained in the framework of protonic conduction but not in the framework of electronic conduction and as such, they constitute additional evidence that melanin is a proton conductor above the percolation threshold.

In summary, from the observed dependence of the conductivity of melanin on hydration, we propose the existence of two different dominant conduction mechanisms, both dependent on hydration. At low hydrations, we advocate electronic

conduction enhanced by an increase in dielectric constant with hydration. Then at hydration levels above the percolation threshold of 10 wt% water, we propose additional protonic conduction. At hydration above 15 wt% water, protonic conduction dominates.

## 7.2 Comparison with Experiments

Our model of a mixed conductor with two hydration dependent charge transport mechanisms is consistent with the results of many experimental studies of melanin. In this model, the low conductivities reported by Jastrzebska *et al.* [1] and Baraldi *et al.* [13] would be electronic as they were measured under vacuum or in the steady state respectively. The higher conductivities reported by Jastrzebska [1] would be mostly protonic as they were measured in hydrated melanin. The two hopping distances measured in the dielectric studies [16] could correspond to the electron hopping distance and the average proton hopping distance at the hydration level of the study. The coulometric study by Powell and Rosenberg [25] proposed protonic conductivity in the same region we do. Additionally, the saturation of the effect of hydration on electronic conductivity at around 10 wt% water is in agreement with the 12.4 wt% monolayer coverage of melanin with water as determined by Powell and Rosenberg [25] from the adsorption isotherm of melanin.

However, there are experimental observations inconsistent with our proposed model. Primarily, the coulometric study [25] did not show an increase in the protonic fraction of the total conductivity with hydration over the 12 to 35 wt% water examined.

## 7.3 Modelling with Equivalent Circuits

Having proposed a possible explanation for conduction in melanin, we have attempted to develop an equivalent circuit model that explains the observed total conductivity including the drop in conductivity between 10 and 15 wt% water. Interestingly, we were not able to model the dip using any simple equivalent circuit, which suggests some more complicated interaction between the two mechanisms is taking place.

In developing the model, we considered alternative combinations of the two pathways. Essentially, both the electronic path  $E$  and protonic path  $P$  were considered to be resistors with a resistance that varied as a function of hydration. We considered both series and parallel combinations of the two pathways. Series combinations of the two pathways requires some kind of coupling between the two mechanisms. At this point we are not concerned with the mechanism of the coupling and simply assume that it is possible since it already must occur at the contacts.

The equivalent circuit that best modelled the observed conductivities is shown

in figure 7.2. Each parallel component in this diagram may be composed of any combination of the electronic and protonic pathways where the total length of each pathway satisfies the proportion  $x_i : (1 - x_i)$ . To calculate the total conductivity in this circuit for any particular  $\sigma_E$  and  $\sigma_P$  we first calculate the impedance of the  $i$ th series pathway  $Z_{Si}$ :

$$Z_{Si} = \text{impedance of electronic section} + \text{impedance of protonic section} \quad (7.5)$$

$$= \frac{L_E}{A\sigma_E} + \frac{L_P}{A\sigma_P} \quad (7.6)$$

$$= \frac{Lx_i}{\sigma_E A} + \frac{L(1-x_i)}{\sigma_P A} \quad (7.7)$$

$$= \frac{L\sigma_E + Lx_i(\sigma_P - \sigma_E)}{A\sigma_E\sigma_P} \quad (7.8)$$

where we have used the definition of conductivity  $\sigma = L/Z A$  where  $Z$  is the impedance,  $L$  is the length of a pathway and  $A$  is the area of a pathway. Assuming that the area of each parallel pathway  $A$  is the same, combining  $N$  series pathways in parallel gives

$$\frac{1}{Z_T} = \sum_{i=1}^N \frac{1}{Z_{Si}} \quad (7.9)$$

$$\frac{NA\sigma_T}{L} = \sum_{i=1}^N \frac{A\sigma_E\sigma_P}{L\sigma_E + Lx_i(\sigma_P - \sigma_E)} \quad (7.10)$$

$$\sigma_T = \frac{1}{N} \sum_{i=1}^N \frac{\sigma_E\sigma_P}{\sigma_E + x_i(\sigma_P - \sigma_E)} \quad (7.11)$$

where  $x_i$  is the  $i$ th element of the vector  $x$  which ranges from 0 to 1 with  $N$  elements.

To find the total conductivity, we used MATLAB to evaluate equation 7.11 at 100 different hydration points summing over 100 parallel pathways. The conductivities at each hydration point  $\sigma_E$  and  $\sigma_P$  were calculated from the fitted Rosenberg and percolation models outlined in chapter 4. In addition to the free parameters implicit in the Rosenberg and percolation conductivity, the number of paths  $N$  in equation 7.11 is also free. However, values of  $N$  greater than 100 produced no noticeable change in the total conductivity so that 100 paths is representative of a great many paths. The total conductivity calculated from 100 paths is plotted in figure 7.3.

Examining figure 7.3, we see that the total conductivity of the melanin samples is modelled quite well in the low and high hydration regimes by the equivalent circuit model seen in figure 7.2 and described by equation 7.11. However, the dip in conductivity between 10 and 15 wt% adsorbed water is not predicted by this model.

Moreover, the dip in conductivity was not explained by any simple equivalent circuit model. A possibility of developing a function for the total conductivity which

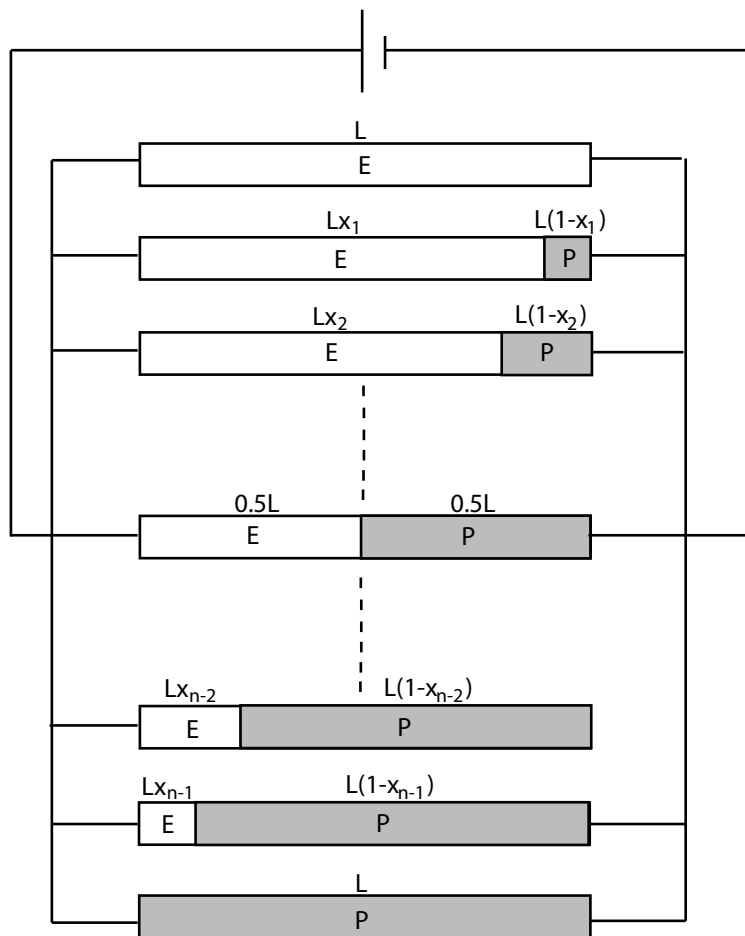


**Figure 7.2:** The equivalent circuit model of the combination of the electronic paths  $E$  and protonic paths  $P$  that may exist in melanin. Resistances of each path are a function of the hydration of melanin.

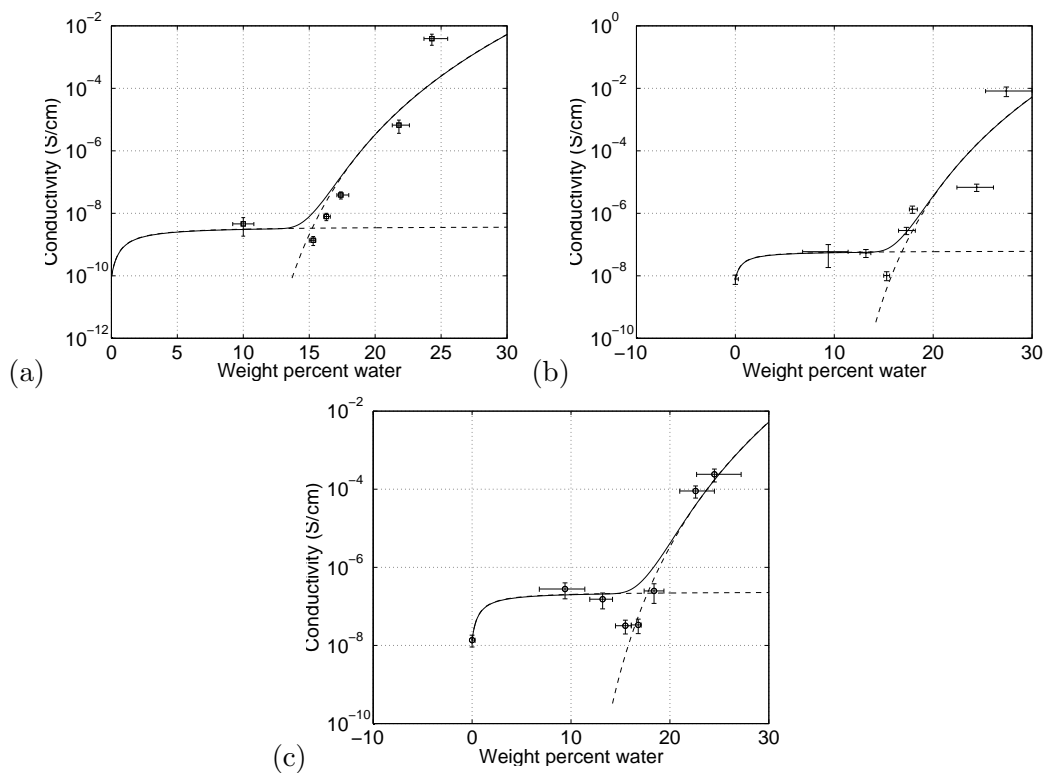


**Figure 7.3:** Model of total conductivity of (a) a 950  $\mu\text{m}$  thick melanin pellet, (b) a 560  $\mu\text{m}$  thick melanin pellet and (c) a 290  $\mu\text{m}$  thick melanin film as a function of hydration. Model given by equation 7.11 based on the equivalent circuit in figure 7.2. Rosenberg and percolation models used in this figure are derived in chapter 4.

includes the dip arises if we introduce some interaction term into equation 7.11. This requires the two mechanisms to interact in some way so that the conduction via one pathway hinders conduction in the other pathway. Although we have not been successful in speculating on what this interaction might be, its existence does fit qualitatively with the observed conductivity; the hydration at which each of the sample's conductivity forms a local minimum corresponds to the point at which the conductivities of the two pathways are approximately equal in magnitude.

## **7.4 Summary**

In this chapter, we developed a full explanation of the conduction mechanisms in melanin which give the experimentally observed relationship between conductivity and hydration first examined in chapter 4. Our proposal of electronic conduction at low hydration and percolated protonic conduction at high hydration is consistent with many charge transport studies on melanin in the literature. Finally, we showed equivalent circuit models predicted the observed behaviour in the low and high hydration regimes but could not predict the dip in the conductivity observed at moderate hydration, suggesting that some interaction term between the two mechanisms is required.

---

# Scanning Electron Microscopy and Thermogravimetric Analysis

---

This chapter presents and discusses the results of two experiments: scanning electron microscopy probing the structure of melanin and thermogravimetric analysis examining the interaction of melanin with water.

## 8.1 Scanning Electron Microscopy

To try to determine the reason behind the similarity in the hydration-dependent conductivity of the melanin films and pellets, we examined the structures of both the pressed melanin powders and electropolymerised films by scanning electron microscopy.

### 8.1.1 Materials and Methods

Samples of pressed melanin powders and electropolymerised films were prepared as in section 4.1.1 but without contacting. Some samples were coated with a 15-18 nm layer of platinum. Samples were observed with a JEOL 6300F scanning electron microscopy with an accelerating voltage of 5 kV.

### 8.1.2 Results and Discussion

Figure 8.1 is a scanning electron micrograph down the edge of an electropolymerised melanin film at a magnification of 20 000 times. We see a layered structure.

Figures 8.2, 8.3 and 8.4 are electron micrographs of a pressed pellet of melanin powder. Figure 8.2 at 1500 times magnification shows the pellet has a predominantly smooth surface. This is in contrast to the slightly granular surface we were expecting to see. Figures 8.3 and 8.4, at 5000 and 20 000 times magnification respectively, show a layered structure similar to that observed in the melanin film micrographs. The

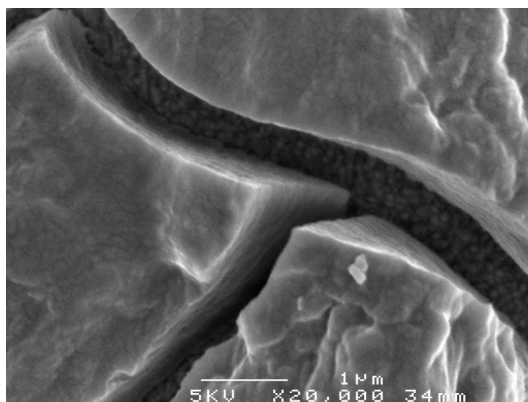


**Figure 8.1:** Scanning electron micrograph down the edge of an electropolymerised melanin film. Sample was coated in platinum. Magnification is 20K. Image taken by Shuzhi Cai.

observation of this structure was very unexpected. Rather, we expected no structure within the pellets.

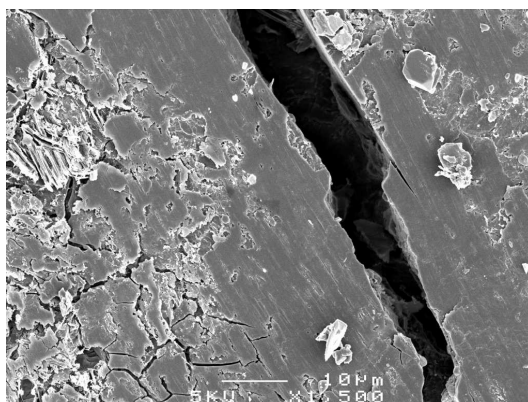


**Figure 8.2:** Scanning electron micrograph of a pressed pellet melanin powder. Sample was coated in platinum. Magnification is 1.5K. Image taken by Shuzhi Cai.

The surprising observation of a layered rather than amorphous structure in the pressed melanin powders suggests that the pellets may have been sintered. Sintering is defined by German [51] as “a thermal treatment for bonding particles into a coherent, predominantly solid structure”. There are methods of pressure-assisted sintering but these usually require temperatures over at least half the melting temperature of the material.[51] Simple die compaction of a powder without thermal treatment, like our treatment of melanin, usually gives overall shape to the powder



**Figure 8.3:** Scanning electron micrograph of a pressed pellet of melanin powder. Sample not coated in platinum. Magnification is 5K. Image taken by Shuzhi Cai.

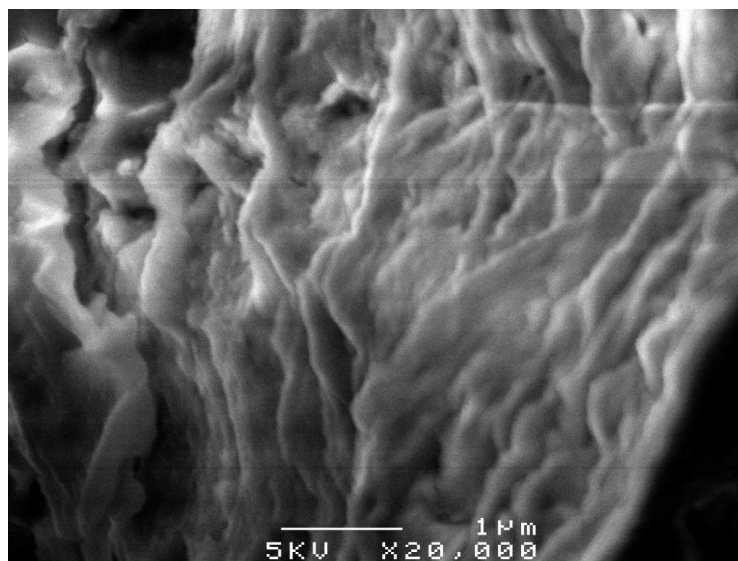


**Figure 8.4:** Scanning electron micrograph of a pressed pellet of melanin powder. Sample not coated in platinum. Magnification is 20K. Image taken by Shuzhi Cai.

by increasing density but does not induce bonding between powder particles.[51] However, the clear layered structure visible in the electron micrographs suggests that local temperatures in the sample under pressure may be high enough to allow viscous flow of the monomer units.

The similarities in the structure and hydration-dependent conductivity of the melanin films and pressed powders indicates that the films may not give any additional information about the properties of melanin. It may be sufficient to just examine pressed powders, which are much easier to synthesis and work with.

## 8.2 Thermogravimetric Analysis

Thermogravimetric analysis (TGA) continually weighs a sample as it is heated at a constant rate. The shape of the resulting map of weight to temperature yields information on the thermal stability of the sample. When performed on hydrated materials, TGA can give an indication of how much water is in the sample and how that water interacts with the adsorbent. We performed thermogravimetric analysis on both the pressed powders and electropolymerised films of melanin.

### 8.2.1 Materials and Methods

#### Sample Preparation

As for the SEM, samples of pressed powders and electropolymerised films were prepared as in section 4.1.1 but without contacting. Before performing running the TGA, samples were stored overnight in a sealed container with saturated sodium chloride solution (relative humidity of about 75.3%). This measure was taken so that the samples were well hydrated at the start of the thermogravimetric analysis.

#### Experimental Method

Thermogravimetric analysis was performed with a ??? thermogravimetric analyser. Samples were initially kept at 25°C for five minutes in ambient humidity. They were then heated from 25°C to 600°C at a rate of 5°C per minute in air atmosphere. To slow the drying rate, no nitrogen flow was used.

### 8.2.2 Results and Discussion

Figure 8.5 shows the weight of the powder and film as the samples were heated. Overall, these thermograms show the masses of both samples decreased significantly so that only about 30% of the initial mass remained at 600°C. Both thermograms, but particularly the film thermogram, are very similar to the thermogram recorded by Deziderio *et. al* for a thin synthetic melanin film synthesised by casting.[52]

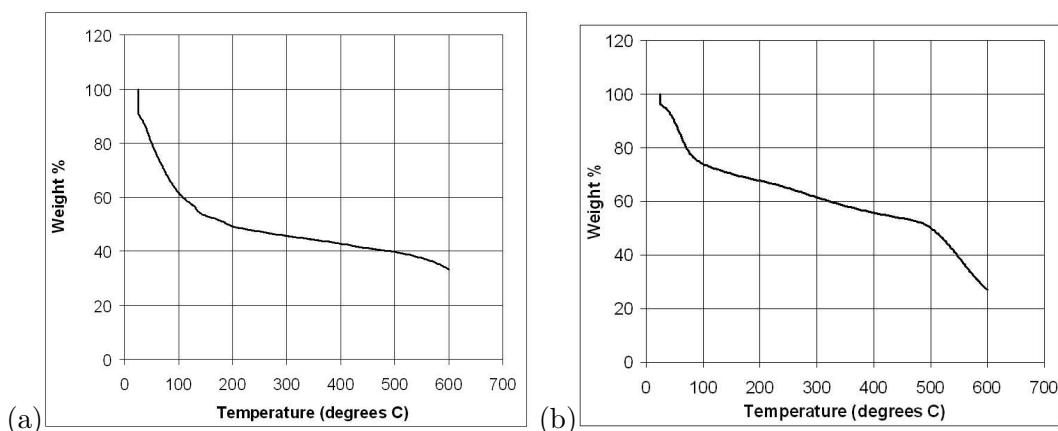


**Figure 8.5:** Thermogravimetric analysis of synthetic melanin (a) pressed powder and (b) electropolymerised film.

In both samples, we see an initial loss of weight while the sample was kept at 25°C which we credit to water desorption.

During the heating phase from 25°C to about 500°C, the pellet displays an exponential-like decay in mass while the thermogram of the film appears to have some extra features in this region: an initial bump then a fairly constant decay. The characteristics of the two curves in this region can be better compared using plots of the derivative of the weight percent with respect to the temperature, against the temperature of the sample seen in figure 8.6. Comparing these figures we see that the characteristics of the two samples are actually quite similar: the masses initially decrease at a fast rate, this rate then slows and becomes almost constant. The main difference between the two samples is the temperature at which the rate of decrease of the mass becomes approximately constant. It occurs at  $\sim 100^\circ\text{C}$  for the film and at  $\sim 200^\circ\text{C}$  for the pellet.

As the samples were heated past 500°C, the masses of both samples decayed at a faster rate. It has previously been proposed from results of TGA [52] and differential scanning calorimetry [15, 52] that melanin is thermally stable up to about 500°C, and that the majority of mass lost at lower temperatures is due to water loss.[15] Our data supports this proposal. The melanin in both the films and pellets does not appear to begin to decompose until about 500°C as indicated by the sharp drop in the mass particularly evident in the film thermogram. As water is the only other substance present in a significant fraction in the sample, the mass lost at temperatures below 500°C must be mostly credited to water loss although there is likely to be a small loss due to low temperature decomposition.

The retention of water in melanin up to about 500°C indicates that some water must be very strongly bound to the melanin.[15] We expect that the vast majority

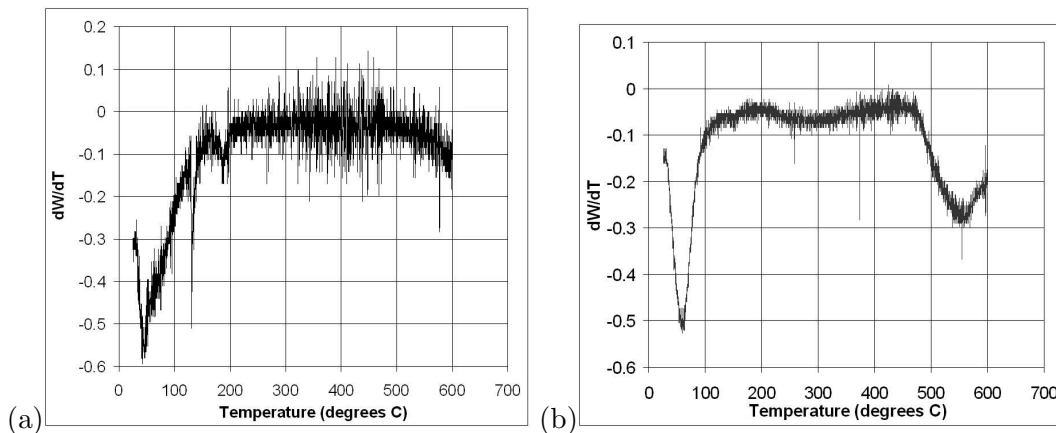


**Figure 8.6:** Derivative of the thermogram from thermogravimetric analysis of synthetic melanin (a) pressed powder and (b) electropolymerised film. The y-axis is the derivative of the weight percent of the sample with respect to temperature where the initial weight of the sample is 100%.

of loosely bound water will have evaporated by 100°C, the boiling point of water. This expectation fits well with our data as both samples show the quickest rate of mass decrease below 100°C and a fairly constant rate of decrease between 100°C and the decomposition temperature of 500°C. Assuming all the mass lost below 100°C is water, then loosely bound water makes up about 40% of the initial mass of the pellet and 25% of the initial mass of the film. Between 100 and 500°C, the mass of the pellet drops a further 20% and the mass of the film a further 25%. At least some of this mass is likely to be additional water which was strongly bound to the melanin.

Overall, if we credit the mass loss between 25°C and 500°C to water loss exclusively, then this suggests that up to 60% and 50% of the initial masses of the pellet and the film respectively (at an initial relative humidity of 75.3%) was water. This is significantly greater than the 25 wt% water measured by Powell and Rosenberg [25] in their isotherm measurements on loose melanin powder at this humidity. This disparity suggests that rather than using the powder isotherm from the literature, we should obtain isotherms for each different sample type.

The similarities in the thermograms of the two sample types fits with our observations of similar conductivities and similar structures. However, the existence of some differences further reinforces the need for individual isotherms for each sample type.

---

## 8.3 Summary

Scanning electron microscopy of the pressed melanin powders and thin melanin films revealed similar layered structures in both samples. A layered structure in the pellet was a surprising result that may be caused by pressure sintering during the pressing process. The structural similarity is the likely reason behind the similarities in the relationship between the conductivity and hydration for each of the samples. Thermogravimetric analysis of the two samples showed similarities in the results from the two samples which are likely to be due to this structural similarity. The thermograms showed that melanin is thermally stable up to about 500°C and adsorbed water may make up about 50% of the weight of hydrated melanin. This water appears to consist of a loosely bound fraction which is lost by 100°C and a strongly bound fraction which can remain in the structure at higher temperatures. The existence of a strongly bound and loosely bound fraction is in agreement with the thermally-stimulated depolarisation current measurements [14] discussed in chapter 2.



---

# Charge Carrier Mobility

---

This chapter outlines an experiment aiming to measure the charge carrier mobility in melanin as a function of hydration.

## 9.1 Materials and Methods

### 9.1.1 Sample preparation

For the mobility measurements, contacts on the melanin were created using the same method followed for the conductivity measurements but with a different contact configuration. In this case, two parallel gold contacts separated by  $(1.17 \pm 0.01)$  mm were evaporated onto the surface of a pressed pellet of synthetic melanin. As before, copper wires were attached to the contacts with conductive epoxy.

### 9.1.2 Measuring Mobilities

In general, mobility experiments involve measuring the time-of-flight (TOF) of pulse-excited charge carriers across a sample  $\tau_{tr}$ . The mobility  $\mu$  can then be calculated using the relation

$$\mu = \frac{d}{\tau_{tr}E} \quad (9.1)$$

where  $d$  is the distance between the contacts where the pulse is created and measured and  $E$  is the electric field in which the charge-carriers move.

Developing a method of measuring the TOF in melanin was difficult due to the nature of the system. If the charge carriers we are attempting to measure the mobility of are protons as we propose, then we expected to run into problems due to space-charge polarisation. We expected this problem to be exacerbated if the concentration of the protons is such that the concentration at the injecting electrode had already decayed before the arrival of the fastest charge-carriers at the rear electrode. These effects result in distorted space-charge-limited TOF pulses.[54] According to Farchioni and Grosso [54], in space-charge limited pulses, the observed

TOF  $t_{SCL}$  is related to the actual TOF  $t_{tr}$  by

$$\tau_{SCL} = 0.786\tau_{tr}. \quad (9.2)$$

We also expected that trapping of protons might be a problem in mobility measurements as protons can bond temporarily with fixed water molecules and ionised melanin molecules. Trapping causes an additional distortion to the TOF pulse as only a fraction of the generated charges actually arrive at the collection electrode. In the worst case scenario of a high concentration of traps, all charge-carriers would be trapped resulting in no observable current at the collection electrode.

Traditional methods of measuring mobility, such as those described by Poplavskyy and Nelson [53] were tried, but were found to be inappropriate as the continuous, externally-applied electric fields required were large enough to dry the sample by resistive heating and ionisation of water. A pulsed drift field may have made these methods feasible but was beyond the scope of this thesis.

As traditional methods did not work, we developed a method for measuring the TOF of protons in the melanin by examining the current transient resulting from the application of a step voltage. The circuit used is illustrated in figure 9.1. A Stanford Research Systmes DG535 Pulse Generator injected a 1V pulse into one electrode on the melanin and a Digital Oscilloscope monitored the resultant voltage across the resistor in series with the sample.

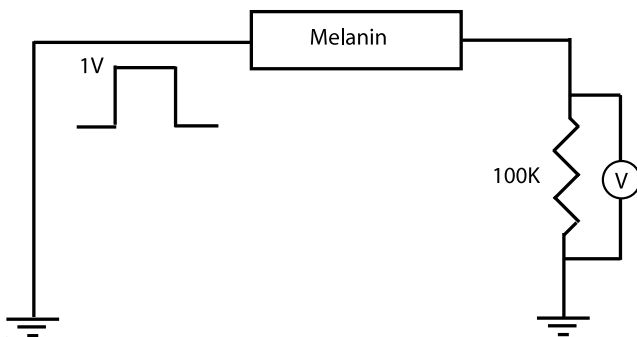


**Figure 9.1:** Circuit used for measuring the time-of-flight of charge-carriers in melanin.

To minimise drying of the sample and the accumulation of a space charge, the measurements were made very quickly after the start of application of the pulses, and the pulse generator was turned off as soon as an oscilloscope screen-shot of the signal was captured.

Similar to the conductivity measurements, humidity was controlled using saturated salt solutions. Both positive and negative injected pulses were examined. The length of the pulses was chosen such that the TOF peak was observable. They ranged between 50ms as 2ms, decreasing and the humidity increased. A 650  $\mu\text{m}$  thick pellet

of pressed melanin powder was the only sample examined in this experiment.

## 9.2 Results and Discussion

Figure 9.2(a) shows the voltage measured across the resistor when a  $500 \mu\text{s}$ ,  $+1 \text{ V}$  pulse was applied to the melanin sample with 15.2 wt% adsorbed water. The peak in the current corresponds to the time of the maximum probability of arrival at the collection electrode. After this time, the current drops due to the accumulation of space-charge and/or a deficit of free protons. This is the same process we proposed in chapter 7 to explain the saturation in the IV curves at low adsorbed water levels. In this way the results of the two experiments corroborate each other. Similar curves were observed with 8.7 and 16.5 wt% adsorbed water.

Figure 9.2(b) shows the voltage measured across the resistor when a 2 ms,  $+1 \text{ V}$  pulse was applied to the sample with 24.2 wt% adsorbed water. As can be seen, no drop in the current with time is now observed in agreement with our expectations from the conductivity experiment. Similar results were obtained with 17.7 and 21.6 wt% adsorbed water.

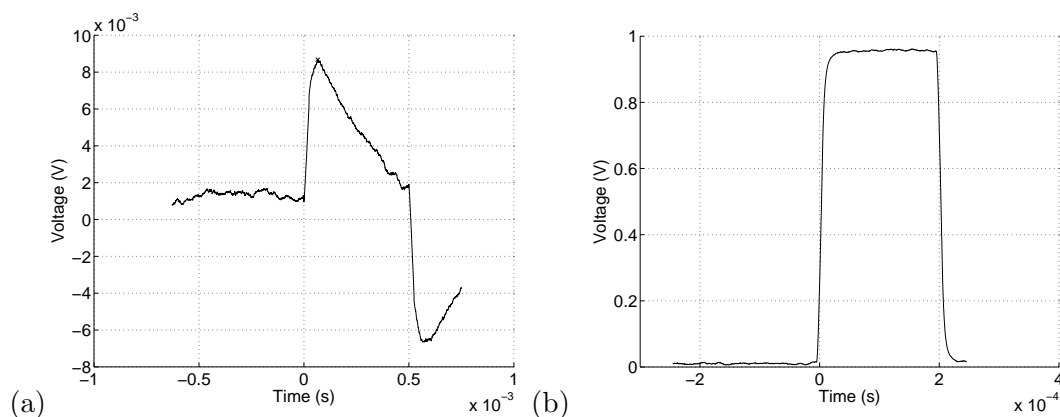


**Figure 9.2:** Characteristic temporal evolution of the voltage across a resistor in series with a melanin sample when a  $+1 \text{ V}$  pulse is applied to the sample with (a) 15.2 wt% water adsorbed and (b) 24.2 wt% water adsorbed. Sample was a pressed pellet of melanin powder. Note the change in y-axis scale. This is why (a) appears noisier.

The hypothesis of an increasing proton current with hydration is supported by the increase in the magnitude of the voltage across the resistor as hydration increases. At low relative humidities, the voltage of  $\sim 10^{-3} \text{ V}$  indicates the melanin is highly resistive so that not many charge carriers arrive at the collection electrode. As hydration increases, a steady rise in the number of charge carriers causes an increase in the current flowing through the resistor resulting in a voltage drop across the

resistor that approaches 1 V, the input voltage.

Pulses of -1 V produced inverted but otherwise identical voltage curves. Again, this may be explained if we assume protons are the dominant charge carriers. Injecting a negative pulse simply forces the protons to travel in the opposite direction giving a negative current.

The time of the maximum probability of arrival at the collection electrode, measured as the time of the peak in the voltage across the resistor, was interpreted as the space-charge-limited TOF  $\tau_{SCL}$ . Hence, the mobility was calculated using

$$\mu = \frac{0.786d^2}{\tau_{SCL}V} \quad (9.3)$$

where  $d$  was the distance between the injecting and collecting electrodes and  $V$  was the applied voltage of +1 V. Mobilities could only be calculated at the three lower hydrations which gave a clear peak in the voltage curve. The mobilities calculated in this manner are listed in table 9.1.

Relative humidity (%)	Wt % adsorbed water	$\tau_{SCL}$ ( $\mu$ s)	$\mu$ ( $\text{cm}^2/(\text{Vs})$ )
$11 \pm 2$	$8.7^{+1.3}_{-0.6}$	$48 \pm 5$	$224 \pm 26$
$33 \pm 2$	$15.2^{+0.1}_{-0.7}$	$66 \pm 10$	$163 \pm 26$
$43 \pm 2$	$16.5^{+0.3}_{-0.4}$	$40 \pm 10$	$269 \pm 69$

**Table 9.1:** Space charge limited time-of-flight of protons  $t_{SCL}$  and corresponding mobility  $\mu$  in melanin at various hydration levels.

Proton mobilities in bulk water and ice are  $3.62 \times 10^{-3}$  and  $0.1 \text{ cm}^2/(\text{Vs})$  respectively [50, 55]. Compared to these figures, our calculated values for the proton mobility in melanin are anomalously high suggesting that we did not measure the true proton mobility. Alternative methods of measuring the mobility will have to be developed to give a better estimate of the true proton mobility in melanin.

### 9.3 Summary

In this chapter, an experiment designed to measure the mobility of protons in melanin as a function of hydration has been presented. When a pulse was injected into the sample with 8.7 wt %, 15.2 wt % or 16.5 wt % adsorbed water, a characteristic temporal evolution of the voltage across the sample was observed. Voltages were typically one one-hundredth of the input voltage indicating little current was flowing through the sample. Unfortunately, interpreting the time of the observed peaks in the voltage as the space-charge limited time-of-flight gives proton mobilities three to five orders of magnitude larger than the proton mobility in liquid water or ice, suggesting that this method does not measure the true proton mobility. How-

---

ever, the shape of the observed voltage pulses and their disappearance at higher hydrations are consistent with the hypothesis of protonic conduction presented in earlier chapters.



---

# Conclusions

---

## 10.1 Further research

The results of this thesis have stimulated many ideas for future research on melanin.

Firstly, improved versions of the conductivity and mobility experiments are necessary to obtain more results so that the ideas discussed in this thesis can be explored and extended. Possible future experiments are:

- Obtaining a better map of conductivity as a function of weight percent of adsorbed water. A stream of air in which the partial water vapour pressure can be controlled, injected into an environmental chamber could be used to obtain a ‘continuous’ data set.
- The development of a better method for measuring the true proton mobility as a function of hydration.
- Obtaining better adsorption/desorption isotherms. This thesis used a single isotherm from the literature. Instead of assuming that the isotherms for the different types of samples are the same, isotherms for each sample type should be measured. Furthermore, surface areas can be calculated from good quality adsorption isotherms and this may provide structural clues. Additionally, isotherms for different adsorbates such as  $N_2$  could provide information on water binding when compared to the  $H_2O$  adsorption isotherms for melanin.

Next, since the suggestion of protonic conductivity in melanin has not previously been explored in any depth, many experiments could be performed that could either confirm or refute its existence. These include:

- Muon spin resonance studies to examine proton diffusion.
- A repeat of the conductivity experiments with deuterated forms of melanin. If protons are important as we suggest, then we expect to get different results with deuterated melanin. In a similar vein, experiments could also be repeated with synthetic analogues eg methoxy...(PIC). As these have fewer protons to donate we expect to see reduced conductivity.

- Characterising the relationship between Hall voltage and hydration. This experiment was attempted in this thesis project but the magnetic fields used were too small to give meaningful results.
- Examining AC conductivity as a function of hydration. AC conductivity measurements can be a better measure of true protonic conductivity as polarisation effects are generally avoided.[37] Alternatively proton injecting electrodes such as platinum electrodes could be used in DC measurements.[37]

Other interesting experiment involving charge transport in melanin include:

- Mapping conductivity v. temperature under vacuum from 1 K to 300 K to definitively show whether Arrhenius-type behaviour is occurring.
- Mapping of conductivity v. temperature at various fixed hydrations from room temperature to 400 K.
- Examining the effect of adsorbed water on photoconductivity.
- Examining the effect of other adsorbates on conductivity. A field effect transistor configuration such as that discussed by Katz [56] may be a useful tool for such studies.
- In the long term, if melanin responds differently to different adsorbates and effect can be sufficiently well characterised, then melanin could be developed into a chemi-sensor.

And finally, from the theory perspective, we should try to determine what the interaction term could be to give the observed drop in conductivity at moderate hydration. Ultimately, we would like to develop a detailed quantitative understanding of transport (both electronic and protonic) in microscopic terms.

Undertaking some or all of this research will further probe the question of charge transport in melanin. However, a definitive answer to this question will require extensive experimental and theoretical work.

## 10.2 Conclusions

This thesis is the first systematic investigation into the mechanisms of charge transport in melanin. In this thesis, relevant literature in a previously disseminated field has been consolidated and several novel experiments probing charge transport have been discussed.

Examination of the conductivity of solid state melanin as a function of hydration revealed a characteristic relationship which holds for both the forms of synthetic melanin tested: pressed powders and electropolymerised films. The similarities in the results from the two different forms of synthetic melanin suggested that the

---

structures of the two samples, originally thought to be quite different, may really be similar. This hypothesis was confirmed by scanning electron microscopy of the two different samples.

Analysis of the observed dependence of the conductivity on hydration suggested that the dominant charge carrier in melanin changes with hydration. In the low hydration regime, between 0 and 10 weight percent adsorbed water, the data fitted with the Rosenberg theory, suggesting that electrons are the dominant charge carriers and hydration increases conductivity by increasing the local dielectric constant of melanin. Above 15 weight percent adsorbed water, a qualitative fit between the data and percolation theory suggested that in this regime, protonic conduction may also occur. In this regime, protons may be transported through a disordered hydrogen-bonded network of water molecules.

Not only was the existence of mixed conduction with a dominant protonic conduction regime shown to be consistent with many of the experimental results from the literature, but it was also shown to reconcile several apparently conflicting results.

Finally, thermogravimetric analysis of the samples indicated that there may be two types of water present in melanin—a strongly bound and a weakly bound fraction. An attempt to measure the proton mobility yielded anomalously high mobility values but did provide some corroborative evidence for protonic conduction.

Overall, this thesis has made one of the first steps on the path to unraveling the charge transport mystery in melanin. Solving this problem is essential for full elucidation of the structure-property-function relationships in melanin.



---

# References

---

- [1] Jastrzebska M, Isotalo H, Paloheimo J, Stubb H. 'Electrical conductivity and synthetic DOPA-melanin polymer for different hydration states and temperatures.' *J. Biomater. Sci., Polym. Ed.* **7**:577-86. (1995).
- [2] Blois MS. 'The melanins: their synthesis and structure.' *Photochem. Photobiol. Rev.* **3**:115-34. (1978).
- [3] Prota G. *Melanins and melanogenesis*. Academic Press, San Diego. (1992).
- [4] Clancy CMR, Simon JD. 'Ultrastructural organization of eumelanin from *Sepia officinalis* measured by atomic force microscopy.' *Biochemistry*. **40**:13353-60. (2001).
- [5] Zajac GW, Gallas JM, Cheng J, Eisner M, Moss SC, Alvarado-Swaisgood AE. 'The fundamental unit of synthetic melanin: a verification by tunneling microscopy of X-ray scattering results.' *Biochim. Biophys. Acta.* **1999**:271-8. (1994).
- [6] Littrell KC, Gallas JM, Zajac GW, Thiyagarajan P. 'Structural studies of bleached melanin by synchrotron small-angle X-ray scattering.' *Photochem. Photobiol.* **77**:115-20. (2003).
- [7] Powell BJ. '5,6-Dihydroxyindole-2-carboxylic acid: a first principles density functional study.' *Chem. Phys. Lett.* **402**:111-5. (2005.)
- [8] Powell BJ, Baruah T, Bernstein N, Brake K, McKenzie RH, Meredith P, Pederson M. 'A first-principles density-functional calculation of the electronic and vibrational structure of the key melanin monomers.' *J. Chem. Phys.* **120**:8608-15. (2004).
- [9] Stark KB, Gallas JM, Zajac GW, Eisner M, Golab JT. 'Spectroscopic study and simulation from recent structural models for eumelanin: II. Oligomers.' *J. Phys. Chem. B* **107**:11558-62. (2003).
- [10] Stark KB, Gallas JM, Zajac GW, Golab JT, Gidanian S, McIntire T, Farmer PJ. 'Effect of stacking and redox state on optical absorption spectra of melanins – comparison of theoretical and experimental results.' *J. Phys. Chem. B* **109**:1970-7. (2005).

- 
- [11] Meredith P, Powell B, Riesz J, Vogel R, Blake D, Kartini I, Will G, Subianto S. 'Broadband photon-harvesting biomolecules for photovoltaics.' In: Collings AF, Critchley C, editors. *Artificial photosynthesis: from basic biology to industrial application*. Wiley, Weinheim. (2005). p. 37-65.
- [12] McGinness J, Corry P, Proctor P. 'Amorphous semiconductor switching in melanins.' *Science*. **183**:853-5. (1974).
- [13] Baraldi P, Capelletti R, Crippa PR, Romeo N. 'Electrical characteristics and electret behaviour of melanin.' *J. Electrochem. Soc.* **126**:1207-12. (1979).
- [14] Bridelli M, Capelletti R, Crippa PR. 'Electret state and hydrated structure of melanin.' *Bioelectrochem. Bioenerg.* **8**:555-67. (1981).
- [15] Simonovic B, Vucelic B, Hadzi-Pavlovic A, Stepien K, Wilczok T, Vucelic D. 'Thermogravimetry and differential scanning calorimetry of natural and synthetic melanins.' *J. Therm. Anal.* **36**:2475-82. (1990).
- [16] Jastrzebska M, Kocot A, Vij JK, Zalewska-Rejdak J, Witecki T. 'Dielectric studies on charge hopping in melanin polymer.' *J. Mol. Struct.* **606**:205-10. (2002).
- [17] Trukhan EM, Perevozchikon NF, Ostrovskii MA. 'Photoconductivity of the pigment epithelium of the eye.' *Biofizika*. **15**:1052-5. (1970).
- [18] Lewis TJ. 'Electronic processes in biology.' *Phys. Med. Biol.* **27**:335-52. (1982).
- [19] Mott N. 'Electrons in glass.' *Rev. Mod. Phys.* **50**:203-8. (1978).
- [20] Deutscher G, Zallen R, Adler J, editors. *Percolation structures and processes*. Adam Hilger, Bristol and The Israel Physical Society, Jerusalem. (1983).
- [21] Stauffer D, Aharony A. *Introduction to percolation theory*, 2nd edition. Taylor and Francis, London. (1991).
- [22] Sahimi M. *Applications of percolation theory*. Taylor and Francis, London. (1994).
- [23] Kirkpatrick S. 'Classical transport in disordered media: scaling and effective-medium theories.' *Phys. Rev. Lett.* **27**:1722-5. (1971).
- [24] Pethig R. *Dielectric and electronic properties of biological materials*. John Wiley and Sons, Chichester. (1979).
- [25] Powell M, Rosenberg B. 'The nature of the charge carriers in solvated biomacromolecules.' *Bioenergetics*. **1**:493-509 (1970).

- 
- [26] Rosenberg B. 'Electrical conductivity of proteins II. Semiconduction in crystalline bovine hemoglobin.' *J. Chem. Phys.* **36**:816-23. (1962).
- [27] Garrett RH, Grisham CM. *Biochemistry*, 3rd edition. Thomson, Australia. (2005).
- [28] Subianto S. *Biological conducting polymers based on melanin*. Honours thesis, Queensland University of Technology. (2003).
- [29] American Society for Testing and Materials. 'F76 Standard test methods for measuring resistivity and hall coefficient and determining hall mobility in single-crystal semiconductors.' *Annual book of ASTM standards*. Philadelphia: ASTM. (2002).
- [30] Runyan WR, Shaffner TJ. *Semiconductor measurements and instrumentation*, 2nd edition. McGraw-Hill, New York. (1998).
- [31] Van der Pauw LJ. 'A method of measuring the resistivity and hall coefficient on lamellae of arbitrary shape.' *Philips Tech. Rev.* **20**:220-4. (1958).
- [32] National Institute of Standards and Technology. *Hall effect measurements*. [Online]. 2002 Nov 12 [cited 2004 Aug 26]; Available from URL: <http://www.eeel.nist.gov/812/hall.html>.
- [33] American Society for Testing and Materials. 'E104-85 Standard practice for maintaining constant relative humidity by means of aqueous solutions.' *Annual book of ASTM standards*. ASTM, Philadelphia. (2002).
- [34] Greenspan L. 'Humidity fixed points of binary saturated aqueous solutions.' *J. Res. Natl. Bur. Stand. Sect. A.* **81A**:89-96. (1977).
- [35] Jastrzebska MM, Jussila S, Isotalo H. 'Dielectric response and a.c. conductivity of synthetic dopa-melanin polymer.' *J. Mater. Sci.* **33**:4023-8. (1998).
- [36] Nelson, DL, Cox MM. *Lehninger Principles of Biochemistry*, 4th Edition. W.H. Freeman, New York. (2005).
- [37] Colomban P, editor. *Proton conductors. Solids, membranes and gels - materials and devices*. Cambridge University Press, Cambridge. (1992).
- [38] Chandra S. 'Fast proton transport in solids.' *Mater. Sci. Forum.* **1**:153-70. (1984).
- [39] Kreuer K. 'Fast proton transport in solids.' *J. Mol. Struct.* **177**:265-76. (1988).
- [40] Walbran S, Kornyshev AA. 'Proton transport in polarizable water.' *J. Chem. Phys.* **114**:10039-48. (2001).

- 
- [41] Careri G, Giansanti A, Rupley JA. 'Proton percolation on hydrated lysozyme powders.' *Proc. Natl. Acad. Sci. USA* **83**:6810-4. (1986).
- [42] Glasser L. 'Proton conduction and injection in solids.' *Chem. Rev.* **75**:21-65. (1975).
- [43] Tomaselli V, Shamos M. 'Electrical properties of hydrated collagen II. Semiconductor properties.' *Biopolymers.* **13**:2423-34. (1974).
- [44] Bardelmeyer GH. 'Electrical conduction in collagen I. Conductivity mechanisms.' *Biopolymers.* **12**:2289-302. (1973).
- [45] Grigera J, Vericat F, Hallenga K, Berendsen H. 'Dielectric properties of hydrated collagen.' *Biopolymers.* **18**:35-45. (1979).
- [46] Ataka M, Tanaka S. 'Electrical conductivity of single crystals of lysozyme.' *Biopolymers.* **19**:669-79. (1980).
- [47] Careri G, Giansanti A, Rupley JA. 'Critical exponents of protonic percolation in hydrated lysozyme powders.' *Phys. Rev. A.* **37**:2703-5. (1988).
- [48] Jastrzebska M, Wilczok T. 'Thermoelectric effect in synthetic dopa-melanins.' *Studia Biophysica.* **122**:39-46. (1987).
- [49] Osak W, Tkacz K, Czternastek H, Slawinski J. 'I-V characteristics and electrical conductivity of synthetic melanin.' *Biopolymers.* **28**:1885-90. (1989).
- [50] Cukierman S. 'Proton mobilities in water and in different stereoisomers of covalently linked gramicidin A channels.' *Biophys. J.* **78**:1825-34. (2000).
- [51] German RM. *Sintering theory and practice.* John Wiley and Sons, New York. (1996).
- [52] FIX ABBREVIATION Deziderio SN, Brunello CA, da Silva MIN, Cotta MA, Graeff CFO. 'Thin films of synthetic melanin.' *Journal of Non-Crystalline Solids.* **338-340**:634-638. (2004).
- [53] Poplavskyy D, Nelson J. 'Nondispersive hole transport in amorphous films of methoxy-spirofluorene-arylamine organic compound.' *J. Appl. Phys.* **93**:341-6. (2003).
- [54] Farchioni R, Grosso G, editors. *Organic electronic materials: conjugated polymers and low molecular weight organic solids.* Springer, Berlin. (2001).
- [55] Pang X-F, Jalbout AF. 'Conductivity properties of the proton transfer exposed in externally applied fields in hydrogen-bonded systems.' *Phys. Lett. A.* **330**:245-53. (2004).

- 
- [56] Katz HE. 'Chemically sensitive field-effect transistors and chemiresistors: new materials and device structures.' *Electroanalysis*. **16**:1837-42. (2004).